State of the Art: Iterative CT Reconstruction Techniques[1]

Lucas L. Geyer, MD[2]
U. Joseph Schoepf, MD
Felix G. Meinel, MD[2]
John W. Nance, Jr, MD[3]
Gorka Bastarrika, MD
Jonathon A. Leipsic, MD
Narinder S. Paul, MD
Marco Rengo, MD, PhD
Andrea Laghi, MD
Carlo N. De Cecco, MD

Owing to recent advances in computing power, iterative reconstruction (IR) algorithms have become a clinically viable option in computed tomographic (CT) imaging. Substantial evidence is accumulating about the advantages of IR algorithms over established analytical methods, such as filtered back projection. IR improves image quality through cyclic image processing. Although all available solutions share the common mechanism of artifact reduction and/or potential for radiation dose savings, chiefly due to image noise suppression, the magnitude of these effects depends on the specific IR algorithm. In the first section of this contribution, the technical bases of IR are briefly reviewed and the currently available algorithms released by the major CT manufacturers are described. In the second part, the current status of their clinical implementation is surveyed. Regardless of the applied IR algorithm, the available evidence attests to the substantial potential of IR algorithms for overcoming traditional limitations in CT imaging.

[1] From the Department of Radiology and Radiological Science, Medical University of South Carolina, Ashley River Tower, MSC 226, 25 Courtenay Dr, Charleston, SC 29425 (L.L.G., U.J.S., F.G.M., J.W.N., C.N.D.); Department of Radiology, Sunnybrook Health Sciences Centre, Toronto, Ont, Canada (G.B.); Department of Radiology, University of British Columbia, Vancouver, BC, Canada (J.A.L.); Department of Radiology, Toronto General Hospital, University of Toronto, Toronto, Ont, Canada (N.S.P.); and Department of Radiological Sciences, Oncology and Pathology, University of Rome Sapienza–Polo Pontino, Latina, Italy (M.R., A.L., C.N.D.).
Received December 17, 2013; revision requested January 15, 2014; final revision received March 18; accepted April 3; final version accepted May 5. **Address correspondence to** U.J.S. (e-mail: *schoepf@musc.edu*).

[2] **Current address:** Institute for Clinical Radiology, Ludwig-Maximilians-University Hospital, Munich, Germany.

[3] **Current address:** The Russell H. Morgan Department of Radiology and Radiological Science, Johns Hopkins Hospital, Baltimore, Md.

Computed tomographic (CT) technology has seen remarkable innovations in the past decade that have substantially improved the diagnostic performance of this modality and steadily increased its clinical indications. Since its first clinical introduction by Sir Godfrey Hounsfield and James Ambrose in 1972 (1,2), the evolution of CT technology has mainly been driven by advances in hardware. During subsequent decades, important milestones have included the introduction of electron-beam CT in the mid-1980s (3), spiral (helical) CT imaging in 1989 (4), and multi–detector row CT in 1998 (5–7). Currently, the major CT manufacturers offer a variety of 64- (8), 256- (9), and 320-detector (10) single-source or dual-source CT systems (11). However, the increased number of detector rows and detector technology are only one domain of CT evolution.

While advances in CT hardware continue to expand the boundaries of physical limitations, increases in computing power have opened additional pathways for improving the performance of this modality via enhanced data processing methods, such as reconstruction techniques. The most prominent example of recent years is the renaissance of iterative reconstruction (IR) CT algorithms. IR approaches are not new and were, in fact, the initially proposed method for data reconstruction in the early days of CT technology during the 1970s (2). However, due to its mathematically demanding properties and the large amount of data in CT imaging, until recently IR has not been practical for clinical purposes. Instead, this reconstruction technique became the default method for nuclear medicine emission tomography imaging modalities with lower spatial and temporal resolution, such as single photon emission CT and positron emission tomography, because of the smaller data volumes and less complex data handling (12). The less perfect, albeit much faster, analytical approach of filtered back projection (FBP) has become the standard reconstruction method for diagnostic CT.

FBP has been established in clinical routine due to its ability to generate CT studies of adequate image quality in a robust and fast manner. Despite its overall acceptable performance, CT studies that are reconstructed with FBP can be affected by high image noise, artifacts (eg, streak artifacts), or poor low-contrast detectability in specific clinical scenarios. For example, data acquisition with reduced tube output or CT imaging of obese patients is often compromised by high image noise; high-density structures, such as calcifications or stents, result in blooming artifacts; metallic implants or bone structures might lead to severe streak artifacts. These particular shortcomings of FBP likely have driven the renaissance of IR algorithms along with general technical evolution providing the required computational power. Furthermore, the increasing number of CT examinations worldwide and the associated radiation dose to the population have clearly fostered the rediscovery of IR technology as a promising tool to decrease radiation requirements via noise reduction.

In this contribution, we review the technical bases of IR and describe the currently available algorithms released by the major CT manufacturers. Further, we survey the current status of their clinical implementation. Regardless of the applied IR algorithm, the available evidence attests to the substantial potential of IR algorithms for overcoming traditional limitations in CT imaging.

Essentials

- Iterative reconstruction (IR) techniques allow for substantial radiation dose savings through noise reduction in CT image processing.
- IR can be used to improve image quality and reduce noise throughout the body, particularly in obese patients.
- Besides improvements in general measures of image quality, an increasing number of reports are emerging on enhanced diagnostic accuracy and artifact suppression with use of IR.
- Special attention should be paid to quantitative CT imaging applications, as the use of IR may alter standards established on the basis of prior analytical image reconstruction methods.
- Robust data regarding the impact and safety of IR in the clinical setting are available; thus, routine implementation of IR in CT protocols should be strongly considered.
- While a multitude of reports highlight the promise of IR to enhance diagnostic performance and reduce radiation at CT, actual examples of adjustment to lower radiation dose settings to fully implement the benefits of IR algorithms in daily clinical practice are still limited.

Technical Background

The exact underlying computational algorithms of the currently available IR algorithms are mostly considered proprietary and only partly revealed by the manufacturers. However, published data indicate that these algorithms can differ substantially with respect to the underlying assumptions of data acquisition, data processing, system geometries, and noise characteristics. Nevertheless, the following sections attempt to provide an objective description of the currently available IR techniques.

Pertinent Principles of CT Data Acquisition

The fundamental goal of CT data acquisition and reconstruction is to as-

Published online
10.1148/radiol.2015132766 **Content code:** CT

Radiology 2015; 276:339–357

Abbreviations:
AIDR = adaptive iterative dose reduction
ASIR = adaptive statistical iterative reconstruction
BMI = body mass index
CNR = contrast-to-noise ratio
FBP = filtered back projection
IR = iterative reconstruction
IRIS = iterative reconstruction in image space
SAFIRE = sinogram-affirmed iterative reconstruction

Conflicts of interest are listed at the end of this article.

sign an attenuation value to each voxel of a three-dimensional volume. Data acquisition is performed by transmitting a fan of photons in multiple angles through the body to an array of detectors. The data at each detector represent the sum of the attenuation of all tissues through which the beam has passed; this is the "raw data." Reconstruction algorithms use the raw data to determine attenuation values for each voxel; differences between reconstruction techniques involve determining how this attenuation value is assigned in the final image. There are two major classes of reconstruction algorithms: analytical and iterative.

Analytical Image Reconstruction–FBP

Knowledge of the basic properties of FBP is crucial to understand the benefits of IR. Analytical reconstruction algorithms such as FBP are based on the assumption that both the measurement process and the projection data are represented by continuous functions. In a simplified model, the x-ray beam is collimated to a pencil shape and moved subsequently parallel to a linear x-ray detector array. Then, the x-ray source is rotated by an angle α and the process is repeated. The intensities measured at the detector are mathematically described as an integral function for a specific angle α and a particular linear shift position of the x-ray tube (Fig 1). The reconstruction process is the solution of the resulting integral equations by inversion (back projection). The back projection that describes the propagation of the measured projection data into the image domain is traditionally combined with a filter component (eg, Ram-Lak filter). The filter compensates for the effect of the so-called low-pass blur that occurs because of the different numbers of projections passing through the center and the periphery of an object. In clinical practice, further variations of the filter (kernels) can be chosen, which are contingent upon a compromise between spatial resolution and image noise. Increasing compensation of the low-pass blur increases the "sharpness" of the image, but also increases image noise. Different kernels enable optimized depiction of soft-tissue or high-contrast structures, such as bone or lung tissue. It is a characteristic of FBP that image sharpness and image noise are directly coupled: The sharper the image, the higher the image noise. With the evolution of CT hardware, adaptations, such as interpolation methods or use of the Feldkamp algorithm or other three-dimensional methods, have been applied to compensate for fan-beam and cone-beam geometries, respectively. Those approaches, however, still remain approximations and interpolations to satisfy underlying assumptions such as a point x-ray source, a pencil x-ray beam, and the point of detector elements, which are prerequisites for the implementation of the Radon transform. The main advantages of this approach consist in its robustness and speed. A major limiting feature of FBP is that it fails to account for image noise that results from Poisson statistical variations in photon number across the image plane; practically speaking, this means that a reduction in radiation dose translates into an increase in image noise. High image noise interferes with the delineation and low-contrast detectability of a structure, so that certain minimal radiation dose requirements need to be fulfilled to generate a diagnostic CT data set. Lowering image noise by choosing "smoother" kernels for image reconstruction will result in impaired spatial resolution with use of a conventional FBP technique.

Figure 1

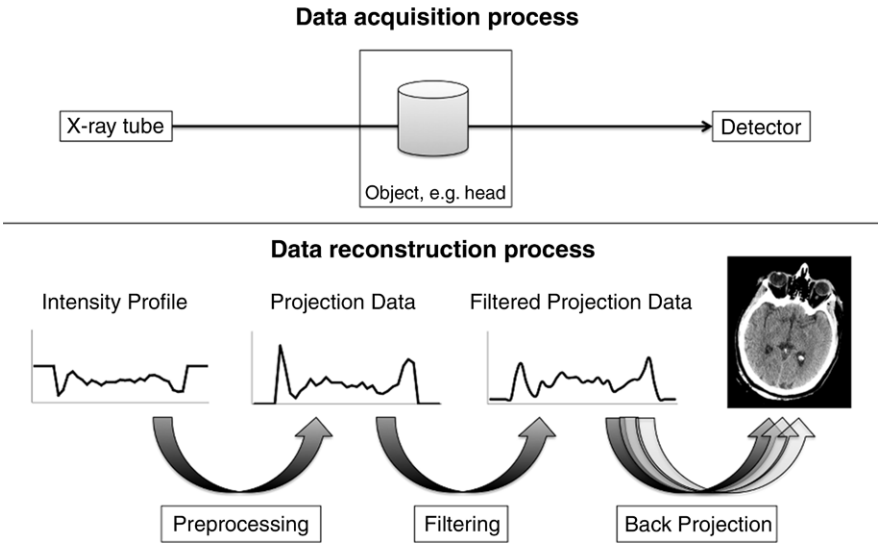

Figure 1: Simplified schematic of CT data reconstruction. Traditionally, several simplifications concerning the data acquisition process are made in the context of FBP: pencil-beam geometry of the x-ray, focal spot as an infinitely small point, intensity measured on a point located at the detector cell center. Regarding a single x-ray, photons with a known intensity are transmitted from the x-ray source through an object to the detector. According to the law of attenuation, the transmitted intensity decreases exponentially due to absorption within the object resulting in a lower measured intensity. Multiple x-rays result in the measurement of intensity profiles in the CT detector. By preprocessing, intensity values are transformed into attenuation values (projection data). Then, projection data are filtered using different reconstruction algorithms (kernels) to create specific image characteristics for soft-tissue or high-contrast visualization. Finally, the measured projection data are propagated into the image domain (back projection). Multiple projections are needed to solve the mathematical system with multiple equations and variables to generate the final CT image.

Iterative Image Reconstruction

In general, the process of data acquisition can be described by the following formula: $p = Hf + n$, where the measured

Figure 2

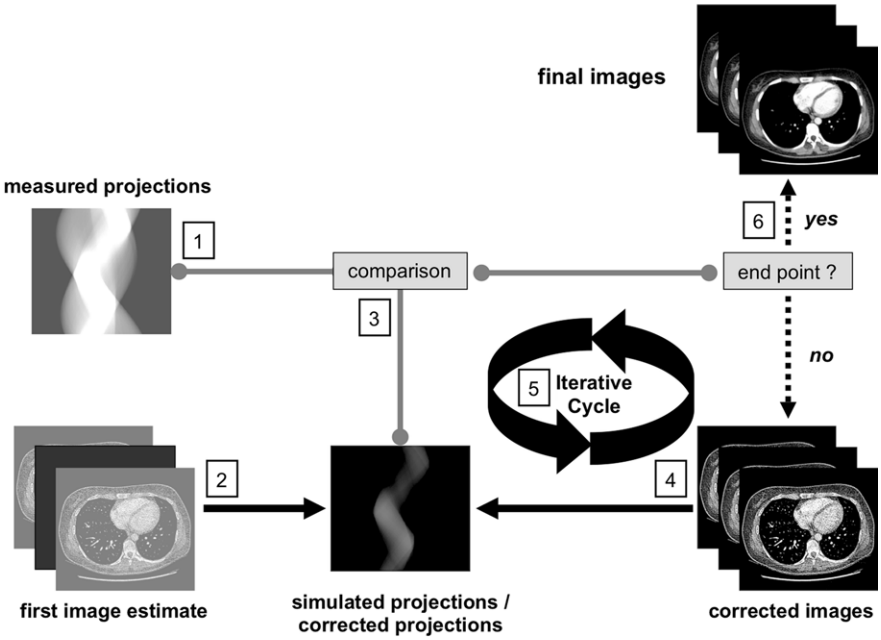

Figure 2: Schematic representation of the principle steps of iterative image algorithms. Following the CT acquisition process (measured projections), a first image estimate is generated. An x-ray beam is simulated via forward projection to obtain simulated projection data, which are then compared with the measured projection data. In case of discrepancy, the first image estimate is updated based on the characteristics of the underlying algorithm. This correction of image and projection data is repeated until a condition predefined by the algorithm is satisfied and the final image is generated.

projection data p is related to the real data f (attenuation coefficient) through a projection process H and the additional noise n. The image reconstruction averages the solution of this equation that can be achieved by two mathematically different iterative concepts: algebraic algorithms and statistical algorithms.

The principle of iterative image algorithms is based on six key steps (Fig 2). For a better understanding of the theory and complexity of iterative image reconstruction, Figure 3 illustrates a simplified model. Leaving additional noise n aside, the algebraic algorithm H solves a simple system of linear equations, where the projection value is the sum of two attenuation coefficients along each projection line. In the early 1970s, the first IR algorithm—algebraic reconstruction technique—was implemented, disregarding the additional noise n. Later on, two modified algorithms were developed to improve the performance: simultaneous iterative reconstruction technique and simultaneous algebraic reconstruction technique. For further details, we refer to previous literature (13–15). However, as computational power was limited in the early days of CT technology, IR algorithms were not practical for clinical application.

The example mentioned above also illustrates that the complexity of IR algorithms rapidly increased when additional components of the data acquisition process or image characteristics were integrated. In addition to different sources of image noise (eg, statistical photon distribution, electronic noise), the geometry of modern CT systems (eg, shape and size of the detector and the focal spot, distances between the x-ray tube, the isocenter, the detector, etc) contributes substantially to the projection process.

Basically, the mathematical model of IR methods consists of two parts: the so-called data term combined with a regularization term (or prior term). While the data term is a fitting model of the observed projection data, the regularization term often incorporates the nonuniformities of the CT system, such as noise. In a so-called statistical IR, a weighting term is introduced into the data term that assigns low weight to data with high statistical uncertainty (high noise) and high weight to data with low statistical uncertainty (low noise). Data fitting can be mathematically achieved by different statistical methods, such as maximum likelihood, least squares, or maximum a posteriori estimators. Variations of both the data and the regularization term result in different characteristics, mainly affecting the handling of image noise and artifacts.

Hybrid Algorithms

So-called hybrid algorithms combine both analytical and iterative methods in different combinations. In one arrangement, the initial image is generated by the use of analytical methods (raw data domain), and iterative methods are focused to optimize image characteristics, for example, noise, in the image domain. In another pairing, an iterative algorithm can be directly implemented into the reconstruction process to focus on image improvements of an initial image estimate that is generated by an analytical method. In the literature, the term *hybrid IR* usually refers to algorithms that mainly decrease image noise by iterative methods. In contrast, the term *model-based iterative reconstruction* usually refers to algorithms that implement models of the acquisition process, image statistics, and system geometry. However, we find it important to emphasize that the clinical performance of IR algorithms is not necessarily related to the complexity of the method. Consequently, we do not further distinguish between both approaches in the clinical section of the manuscript. Currently commercially available IR algorithms are utilizing a broad spectrum of the above-described principles.

Figure 3

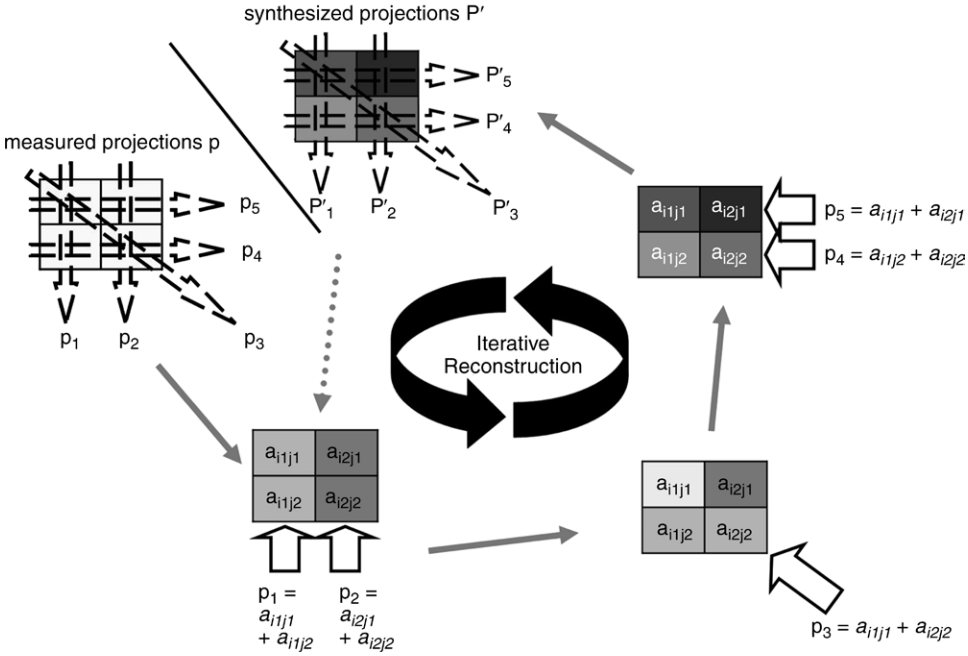

Figure 3: Simplified model of an algebraic IR cycle. Four different attenuation coefficients, in a 2 × 2 pixel matrix, are represented by five projections *(p)* at three different angles (two acquired in horizontal, two in vertical, and one in oblique directions). The matrix is successively updated by stepwise back projection. The corrected attenuation coefficients can be used to generate synthesized projection data *(P′)* via forward projection. A subsequent cycle can be initiated until a stop criterion is satisfied.

Vendor-specific IR Approaches

GE Healthcare

Adaptive statistical iterative reconstruction.—In late 2008, GE Healthcare (Waukesha, Wis) introduced their first hybrid adaptive statistical iterative reconstruction (ASIR) algorithm for clinical use (16). ASIR, unlike FBP, performs reconstruction of the CT data sets by modeling the system statistics in the process (17–21), using information obtained from the FBP algorithm as a building block for each individual image reconstruction. The ASIR model integrates matrix algebra to convert the measured value of each pixel to a new estimate of the pixel value. This pixel value is then evaluated and is compared with the ideal value that is predicted with noise modeling. The process is repeated in successive iterative steps until the final estimated and ideal pixel values ultimately converge. ASIR is blended with traditional FBP in 10% increments according to user preference. However, similar to other IR techniques, a higher percentage of ASIR in the reconstruction can result in degradation of image quality, with a somewhat unfamiliar, almost "plastic" texture to the images (22,23).

Veo.—Veo, initially introduced as model-based iterative reconstruction, is the second-generation IR algorithm introduced by GE Healthcare (24). The calculation process of Veo is complex and exceeds the scope of this article. We therefore refer to the publications by Yu et al (25) and Thibault et al (26) for more detailed descriptions. In brief, this algorithm incorporates an extensive three-dimensional model of the data acquisition process, including system optics (eg, geometry of the x-ray source, cone-beam shape, detector characteristics), in addition to the models of the statistical noise and the prior term. The model of the system optics describes how each element of a scanned object is projected onto the detector, disregarding the simplified assumptions of FBP. Veo assumes a three-dimensional volume of each voxel element and takes a focal spot with known dimensions, as well as an active area of the detector, into account. Veo also models the statistical distribution of the measured data from the physics of the interaction of x-rays with matter. Similar to other IR solutions, parts of model-based iterative reconstruction can be initialized with a FBP reconstruction to facilitate a relatively fast convergence. Then, all voxels of the image volume are updated within one complete iterative cycle. This extensive modeling and its complexity are demanding on computational power and time; currently, reconstruction times range between 10 and 90 minutes depending on the number of images, which roughly equals 0.2 to 0.5 images per second (27). This potential delay between data acquisition and availability of images for interpretation has to be considered in clinical practice, for example, for emergent indications.

Philips Healthcare

iDose⁴.—In 2010, Philips Healthcare (Best, the Netherlands) introduced their approach to IR techniques with iDose⁴. The iDose⁴ reconstruction algorithm first analyzes the projection data, identifying and correcting the noisiest CT measurements (poor signal-to-noise ratio or very

low photon counts). A model including the photon statistics is applied to each projection for the detection of very noisy measurements. Through an iterative process, the noisy data are penalized and edges are preserved. This process ensures that the attenuation gradients of underlying structures are retained, thus preserving spatial resolution while allowing a substantial noise reduction. The noise left after this process is propagated to the image space; however, the propagated noise is highly localized and can be removed to support the desired level of dose reduction. This technique aims at preventing photon starvation artifacts (streaks, bias) before image creation and maintaining image quality while avoiding the artificial appearance of images that has been typical of earlier generation IR techniques.

From an operative point of view, the percentage of dose reduction (from 0% to 80%) should be chosen before the acquisition, while iDose^4 reconstruction levels (from 0 to 7) can be selected before the scan or after the acquisition of raw data. To maintain the same image quality and noise of FBP, a proportional iDose^4 level should be selected according to the chosen percentage of dose reduction (28). However, a higher iDose^4 level can be applied to increase image resolution. Consequently, the user is able to prioritize a goal of dose reduction, image quality improvement, or a weighted compromise between both goals (29).

Iterative model reconstruction.—Iterative model reconstruction is the second-generation IR algorithm introduced by Philips Healthcare in 2012. In contrast to iDose^4, iterative model reconstruction aims at accounting for not only the noise behavior of the image but also the data statistics, image statistics, and system models during its iterative cycle (30). To our knowledge, however, as of the time of this writing further details about this very recently introduced algorithm have not yet been made available in the imaging literature.

Siemens Healthcare

Iterative reconstruction in image space.—In 2008, Siemens Healthcare (Forchheim, Germany) released their first-generation iterative reconstruction algorithm, iterative reconstruction in image space (IRIS) (31). This approach is based in the image domain, where an initial image is reconstructed from the raw data upon which three to five iterations of the algorithm are then applied, with the goal of reducing noise and enhancing object contrast step-by-step.

Sinogram-affirmed iterative reconstruction.—Sinogram-affirmed iterative reconstruction (SAFIRE) is the second-generation IR algorithm released by Siemens Healthcare in 2010, which incorporates an IR technique that utilizes both raw data and image data iterations with up to five strength levels available for adaptation of the regularization term to control for image impression and noise reduction. The strength is not related to the number of iteration loops (32).

Similar to traditional IR, SAFIRE performs an initial reconstruction using a weighted FBP, after which two different correction loops are introduced into the reconstruction process. In the first loop, new synthetic raw data (from a forward projection) are compared with the original raw data to derive correction projections that are then used to reconstruct a correction image. The detected deviations are again reconstructed using the weighted FBP, and the loop is repeated a number of times depending on the scan mode. The second correction loop occurs in image space, where noise is removed from the image through a statistical optimization process. Noise can be locally estimated and removed by using a dynamic raw-database noise model that, during each iteration, predicts the variance of the image noise in different directions in each image pixel and adjusts the space-variant regularization function correspondingly. Noise reduction occurs almost solely in image space, thus reducing the requirement to return to raw data space. The corrected image is compared with the original, and the process is repeated a number of times depending on the examination type (33,34). SAFIRE can reconstruct up to 20 images per second (35), allowing the reconstruction of a typical thorax examination of 30 cm in 15 seconds.

Advanced modeled iterative reconstruction.—Recently, Siemens released their third-generation IR algorithm. Advanced modeled iterative reconstruction comprises three modifications, compared with previous algorithms (36): *(a)* the use of a weighted FBP in the loop, which aims at improved removal of artifacts based on geometrically nonexact reconstruction operators; *(b)* computations commence with up to two iterations, with the goal of removing geometric imperfections such as cone-beam artifacts; *(c)* the statistical modeling performs a local signal-to-noise ratio analysis to decompose data into information and noise according to the model. Compared with SAFIRE, the analysis incorporates not only nearest-neighbor data but also a larger area.

Toshiba Medical Systems

In the initial IR algorithm developed by Toshiba Medical Systems (Otawara, Japan), adaptive iterative dose reduction (AIDR), the image noise reduction occurred in the reconstruction (image) domain. This IR technique required that the original high-noise images undergo several loops of iteration to reduce the image noise until the desired noise level is achieved (37,38). More recently this technique has been replaced by an AIDR system using a three-dimensional processing algorithm (AIDR 3D) (39). This reconstruction algorithm is based on IR performed not only in the reconstruction domain but also in the raw-data domain. In the raw-data domain, AIDR 3D processing takes into consideration the quantum noise derived from the amount of x-ray photons that reach the detector and the electrical noise from the CT system; the algorithm also uses the raw-data domain in a model accounting for the specific scanner geometry and a statistical noise model to reduce noise (37,40). Finally, in an effort to maintain the noise granularity and render the image more "natural," a weighted blending is applied to the original reconstruction and the output of this iterative process (41).

Clinical Applications

The current evidence on the clinical implementation of IR into CT protocols shows substantial promise for major improvements in image quality, chiefly noise reduction—with subsequent radiation dose reduction—and artifact suppression. The former suggests the opportunity for substantial radiation dose savings by mitigating the contrarian relationship between dose and noise that governs the use of FBP. However, exact estimates of dose reduction in clinical practice are difficult to derive from published data because studies comparing various IR algorithms of the same vendor are scarce and comparisons of different vendors are largely missing. This may be partly due to the fact that virtually all IR techniques are vendor-specific with limited applicability to other CT systems. As expectations concerning image quality can substantially differ between institutions, careful attention to specific data acquisition protocols is required when reviewing literature about IR technology.

Furthermore, recent data indicate that also acquisition parameters of FBP protocols could be improved by means of quality management, such as periodical audits (42). Consequently, the impact of IR in terms of radiation dose reduction might be partly overestimated. One should also keep in mind that there is neither an official definition of terms such as *low dose* or even *ultra-low dose*, which are frequently used in connection with IR techniques, nor a consensus on the best indicator (CT dose index, dose-length product, size-specific dose estimate, etc) of radiation dose (43). Moreover, the current literature on IR technology in CT imaging is mainly focused on image quality and radiation dose. However, investigations of the diagnostic performance of IR and the resulting clinical outcome are largely missing.

Practical Considerations

From a practitioner's point of view, the integration of IR does not introduce major workflow changes as compared with the use of FBP. After data acquisition, the technologist simply selects the appropriate IR reconstruction algorithm (kernel) and the desired strength level (ASIR, iDose^4, SAFIRE), if applicable. Except for Veo—which is currently only available with a standard soft-tissue kernel—all IR algorithms can be combined with a specific reconstruction algorithm, for example, soft tissue, bone, lung, et cetera. In general, the choice of the IR algorithm and its strength level, if available, influences the image impression and noise characteristics. As a result, the selection of the institutionally preferred IR technique is a specific clinical task germane to the individual preferences for image quality: For instance, a more aggressive noise reduction may be beneficial for the detection of low-contrast structures such as hypovascular liver lesions, whereas CT angiography examinations may benefit from strategies aiming at improving spatial resolution or decreasing artifacts, rather than noise reduction. With first-generation IR algorithms in particular, a substantial noise reduction might be associated with an "oversmoothing" of the image, leading to a blotchy appearance of the IR-reconstructed studies (22,23). In addition, second-generation IR algorithms allow for a more effective artifact reduction, such as streak or metal artifacts. However, these effects are not necessarily related to the complexity of the IR algorithm. A practical consideration is that because of the possibly unfamiliar overall image impression, radiologists might initially feel inclined to reject the routine implementation of IR algorithms and question their diagnostic accuracy compared with traditional FBP techniques. Commonly, however, such concerns will be dispelled after an initial learning curve and increasing familiarity with the IR image impression.

Phantom Experiments

Initial reports on the various IR products were largely based on studies in which phantom models were used. Given the purported benefits of IR, studies generally compared some combination of various image-quality parameters, including noise, signal-to-noise ratio, contrast-to-noise ratio (CNR), low-contrast visualization, and spatial resolution. Ghetti et al (44,45) used Catphan (The Phantom Laboratory, Greenwich, NY), a specific phantom for the evaluation of medical imaging equipment, and dedicated three-dimensional spatial resolution phantoms to compare FBP with IRIS and SAFIRE, respectively, and found that both Siemens products preserved spatial resolution while decreasing image noise when radiation dose was kept constant. Attenuation values were unchanged between the IR and FBP algorithms, which led to proportionally increased CNR and low-contrast resolution when the iterative techniques were used. SAFIRE has the ability to vary the iterative strength level from 1 to 5, and the authors found that image noise reduction increased from 10% to 60% with increased strength. Similar studies comparing FBP with AIDR (37) and iDose (46) also found that the iterative products preserved spatial resolution while decreasing image noise when identical acquisition parameters were used. iDose^4 provided image noise reduction of 11%–55%, depending on the iDose level, which resulted in improved low-contrast resolution compared with FBP acquired at the same dose level and equivalent low-contrast resolution compared with FBP acquired at lower doses. AIDR, which does not provide the option to select between different iterative strengths, provided noise reductions of 35%–44%. A more recent study by Mieville el al (47) compared ASIR, Veo, iDose^4, and FBP and reported that the model-based IR product, Veo, resulted in superior image quality compared with the other three techniques, particularly with respect to spatial resolution. The authors further describe improved low-contrast detectability with this algorithm, even at decreased radiation dose levels.

In addition to more visually recognizable methods, a valuable parameter for the evaluation of image quality with IR is the noise power spectrum (NPS). The NPS graphically represents both image noise (defined by the area under

the curve) and noise texture (reflected in the shape of the curve). Most IR algorithms affect NPS graphs similarly—the area under the curve (noise) is reduced while the peak of the curve shifts toward lower frequencies. This particular effect is specifically reported with the use of several IR techniques, including ASIR and Veo (47), IRIS (44), SAFIRE (45), and iDose[4] (46). The perceived consequence is an unfamiliar visual appearance that is commonly described as plastic-like, paint-brushed, blurry, blotchy, or over-smoothed, which can be objectified by NPS analysis (45). IR-FBP blending and variable user-specified iterative strength levels are two techniques the vendors have utilized in their attempt to mitigate this unfamiliar and often undesired textural alteration.

Overall, phantom models have verified the feasibility of IR techniques in reducing image noise while maintaining other image quality parameters, and these studies have led to an ever-expanding body of literature demonstrating similar findings in vivo.

Head and Neck

IR use in the head and neck has shown utility in decreasing dose, improving image quality, and mitigating artifacts (Fig 4). At least two studies demonstrated a reduction in radiation dose associated with cervical spine CT to a level comparable to that of conventional radiography in trauma patients (48,49). Radiation dose decreases in the brain ranging from 20% to 40% have been shown by using ASIR, iDose, IRIS, and SAFIRE (50–54). CT brain perfusion imaging, traditionally associated with relatively high radiation doses, may be well suited to exploit this benefit, with initial studies showing dose reductions of 20% (55). Model-based IR has shown improved delineation of small arteries that are traditionally difficult to image, including arteries within the posterior fossa (56), the anterior spinal artery (57), and the artery of Adamkiewicz (58). SAFIRE utilization in cervical spine CT has resulted in better depiction of the intervertebral disks and ligaments (59,60). Fine bone structures, such as the temporal bone or paranasal sinuses, often necessitate thinner section reconstructions that are subject to increased noise secondary to quantum mottle; again, this has shown to be an area in which the noise-reduction properties of IR techniques may be put to good use (61,62). ASIR has been shown to enhance the delineation between white and gray matter (63). Finally, model-based IR products (such as Veo) or those containing specific metal artifact-reduction algorithms can substantially reduce common artifacts in head and neck imaging, such as photon starvation caused by the shoulders and streak artifact caused by dental hardware (64,65) (Fig 5).

Figure 4

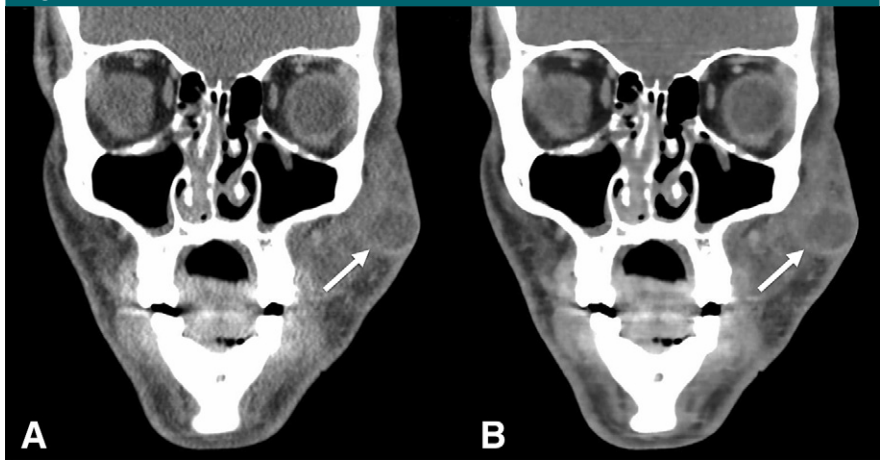

Figure 4: Coronal reformations of contrast-enhanced CT study of the head in a patient with subcutaneous abscess in the left cheek. Compared with, *A,* FBP, the visualization of the abscess formation is improved by noise reduction with use of the, *B,* Veo IR algorithm. The surrounding abscess membrane is clearly depicted (arrow).

Figure 5

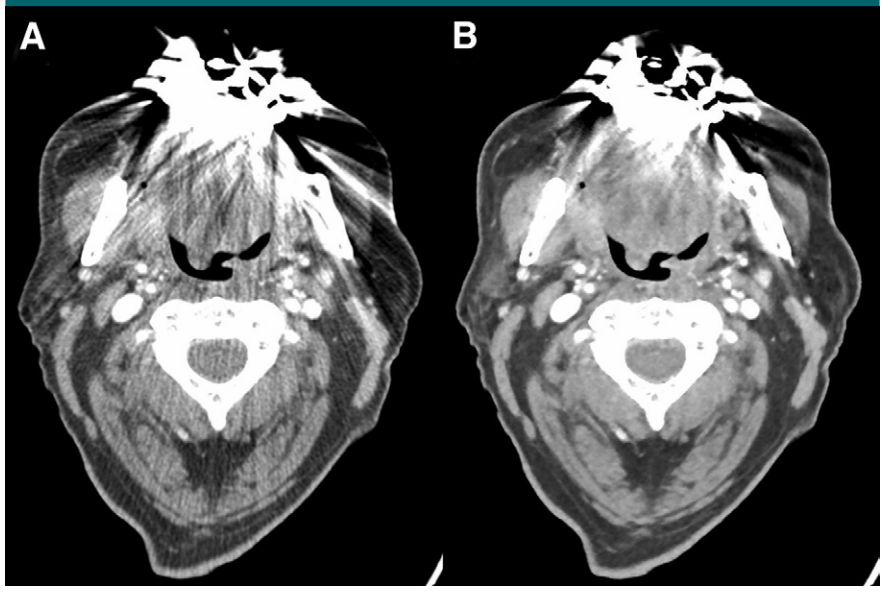

Figure 5: Transverse sections from a CT angiographic study of the carotid arteries in a patient with metallic dental hardware. Compared with, *A,* FBP, there is a reduction of metal artifacts with use of the, *B,* Veo IR algorithm.

Thorax

Currently available IR products have consistently been shown to allow radiation dose reductions without compromising the diagnostic image quality of routine chest CT, with reported dose reductions ranging from 27% to 80% (28,66–73). One group described that Veo was able to depict pulmonary nodules despite radiation dose reductions to levels comparable to those of conventional chest radiographs (74). Studies evaluating IR in thin-section pulmonary CT examinations have shown similar results, with comparable or superior image quality of IR compared with traditional FBP reconstructions (73,75,76) (Fig 6). One study concluded that CT images reconstructed with IR result in better visual scores than conventional FBP reconstruction for the assessment of lung architecture, such as interlobular septa, the centrilobular region, and small bronchi/bronchioles; IR was also superior at delineating pathologic findings such as reticulations, tiny nodules, altered attenuation patterns, and bronchiectasis (77). Similar findings have been observed in a pediatric patient population with cystic fibrosis (78).

While IR may allow greater consistency of emphysema quantification at low-dose CT (79), another study showed that quantitative measures of emphysema and air trapping are substantially influenced by IR algorithms (80). This highlights an important point regarding IR—anything that significantly alters image reconstruction has the potential to influence quantitative methods, potentially arriving at diverging results when compared with standards set by using FBP. Fortunately, this seems not to be the case in one of the most typical applications of IR in thoracic CT, pulmonary nodule assessment. Both phantom-based (81,82) and in vivo studies (29) have suggested that lung nodule volumetry is robust and reproducible throughout a wide range of tube voltage and tube current-time product exposure settings. Furthermore, IR utilization does not negatively affect the performance of lung nodule computer-aided detection systems (83). From a qualitative standpoint, CT imaging with IR maintains diagnostic accuracy compared with FBP in the identification and characterization of ground glass opacities, part-solid nodules, and solid nodules, while allowing a dose reduction of approximately 75% (84,85).

IR has shown considerable potential in CT pulmonary angiography, with estimated radiation savings of 25%–40% (66,70) (Fig 7). While no studies have compared the accuracy of IR versus FBP CT pulmonary angiography in the detection of pulmonary emboli, researchers have shown preservation of reader confidence, with no change in the rate of nondiagnostic studies (86). Indeed, there may be a role for

Figure 6

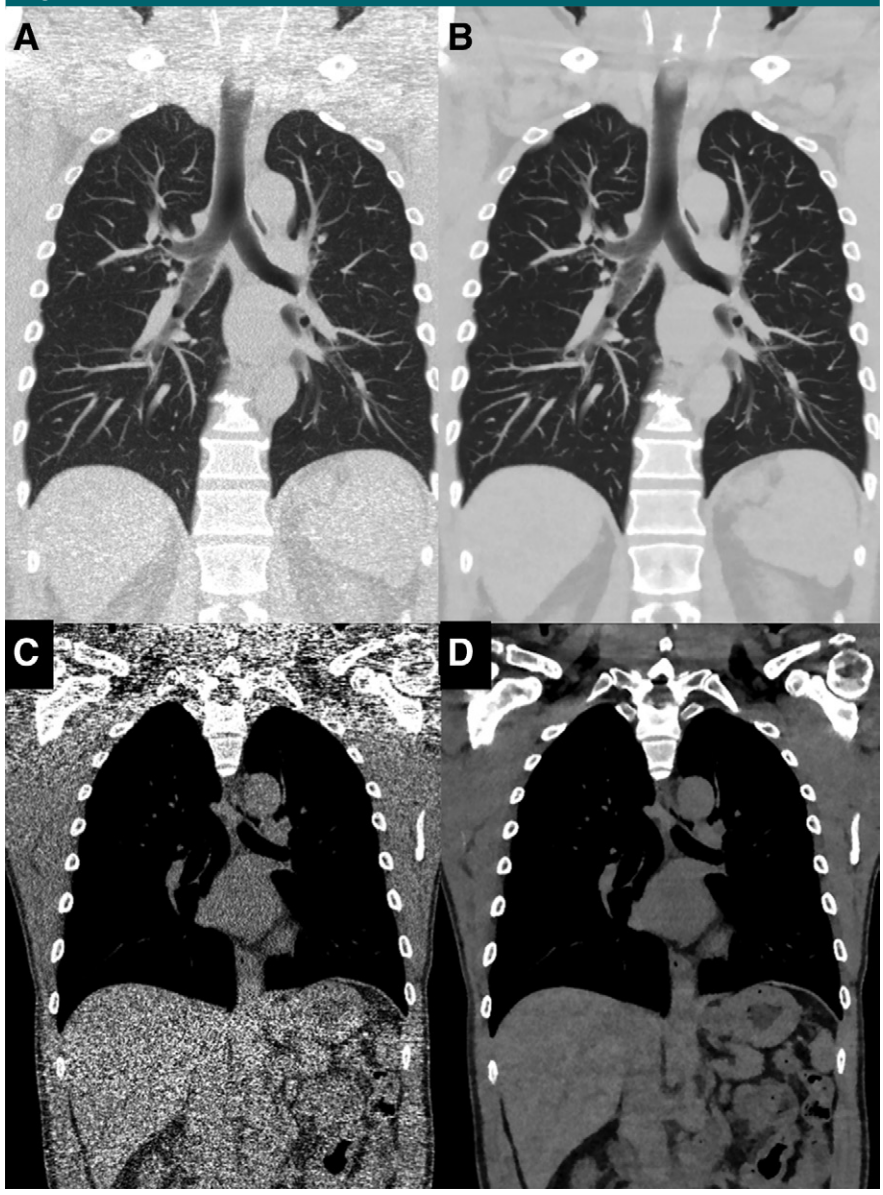

Figure 6: Coronal reformations of nonenhanced chest CT study (effective dose, 1.1 mSv) reconstructed with, *A, C,* FBP and, *B, D,* iDose. In the study using IR, the overall image quality is improved and beam-hardening artifacts at the level of the shoulders are reduced. (Image courtesy of D. Utsunomiya, MD, Faculty of Life Sciences, Kumamoto University, Kumamoto, Japan.)

Figure 7

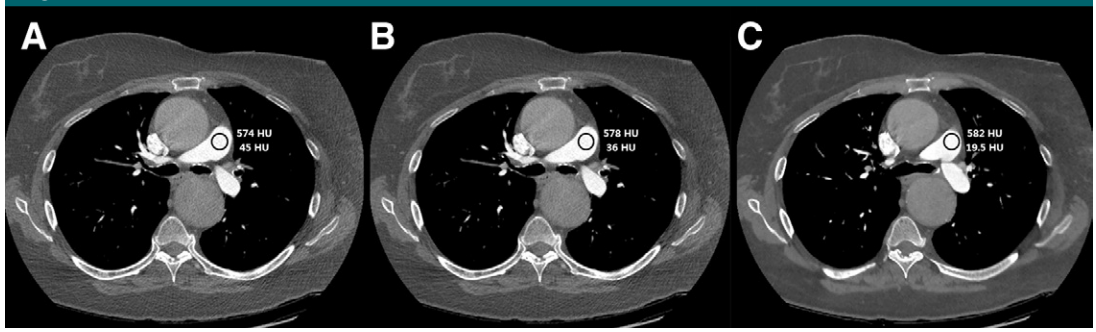

Figure 7: Transverse sections from a CT pulmonary angiographic study displayed at the level of the pulmonary trunk. Compared with, *A,* FBP, the use of, *B,* ASIR results in noise reduction and slightly enhanced CT attenuation. A further enhancement of the visual image quality impression is achieved with, *C,* Veo.

image quality optimization with use of IR in CT pulmonary angiographic examinations independent of radiation dose, for example, in larger patients in whom high noise levels limit the interpretability of small subsegmental pulmonary arteries. Researchers have advocated the use of higher strength IR in these patients to reduce the likelihood of a noninterpretable examination. Of note, while there is concern regarding the undesirable textural effects seen in images reconstructed with high-strength IR, the effect on image quality has been reported to be more modest for vascular structures than for the pulmonary parenchyma itself (70,87).

Cardiac Imaging

Like other applications, the major demonstrated benefit of IR in coronary CT angiography to date has been a reduction in image noise without substantial effects on attenuation compared with FBP reconstructions of the same data. This results in improvements in subjective image quality and vessel assessment (22,35,87–96) (Fig 8). These findings were reported for all commercially available IR products except for Veo, with which experiences are limited to date. For coronary CT angiographic studies, AIDR has shown improved objective and subjective image quality with simulated half-dose acquisitions compared with full-dose FBP reconstructions of the same data (97). Likewise, improved image quality at a dose reduction of 25% compared with FBP have been reported for ASIR (70), and equivalent diagnostic accuracy and image quality with dose reductions up to 72% have been demonstrated (98). Clinical observational studies after implementation of ASIR report 44%–54% reductions in effective dose with cardiac CT applications (87,89). Reduced-dose protocols using IRIS have shown improved image quality compared with routine acquisitions using FBP, with dose savings up to 62% (93); likewise, SAFIRE demonstrated improved image quality compared with FBP with simulated dose reductions of 50%–80% (35,99). Radiation reductions of 55%–63% have been reported without compromising image quality using both fixed- and adaptive-dose protocols with iDOSE reconstructions (90,91,100).

Body mass index (BMI)-adaptive reconstructions using predefined acquisition settings based on patient body habitus offer a potential solution (92,98), while other groups have proposed patient-specific adaptive-dose procedures that adjust scan settings on the basis of allowable image noise (70,101). In this regard, Yin et al (102) recently demonstrated that in a population with a broad range of BMI values, the use of IR after applying a 50% tube current reduction for every selected kilovoltage preserves image quality and diagnostic accuracy at coronary CT angiography compared with standard FBP.

In addition to noise and dose reduction, early evidence suggests that IR products may have a role in reducing beam-hardening and blooming artifacts associated with coronary artery stents and heavily calcified vessels. Reductions in measured stent volumes indicating less blooming artifacts and image noise have been reported along with improved in-stent visualization (93,103–105), and the noise-reduction properties of IR may allow increased utilization of high-resolution (ultrathin section, usually 0.23-mm spatial resolution) coronary CT in-stent evaluation. Traditionally, these examinations are limited by high levels of noise secondary to photon starvation. Early studies have shown improvements in noise, blooming artifacts, in-stent visualization, and diagnostic accuracy with use of IR in conjunction with high-resolution reconstruction kernels and acquisitions (106–108). Likewise, Renker et al (109) compared IRIS to FBP in patients with Agatston scores of 400 or greater and showed that IRIS resulted in significantly lower image noise (P = .011–.035) and calcification volume (P = .019 and .026), significantly higher subjective image quality (P = .031 and .042), and significantly improved per-segment diagnostic accuracy for detection of significant stenoses (P = .0001), with overall diagnostic accuracy of 95.9% for IRIS, compared with 91.8% by using FBP. Note that these reductions in calcium volume may be a relevant consider-

Figure 8

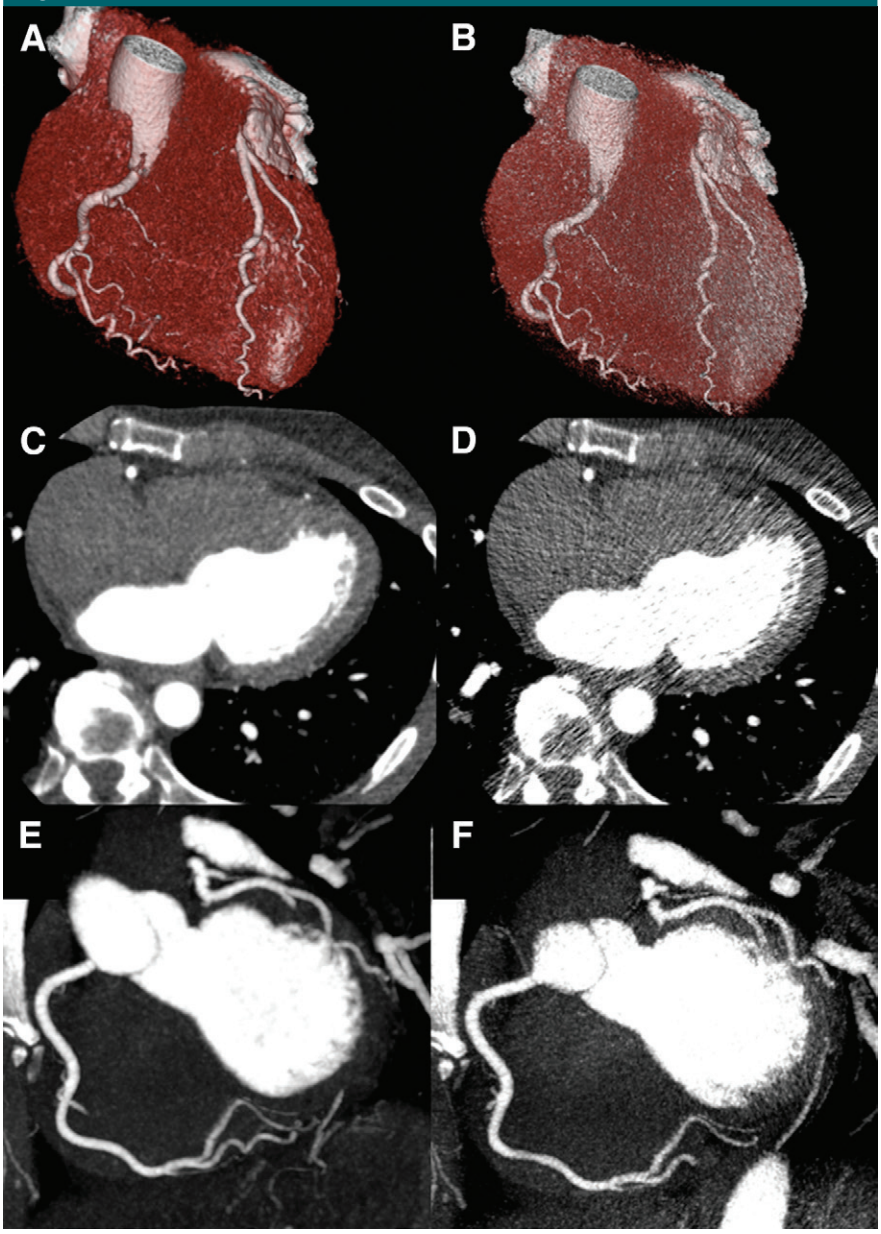

Figure 8: *A, B,* Three-dimensional volume-rendered reconstructions, *C, D,* transverse sections, and, *E, F,* oblique maximum intensity projections of a coronary CT angiographic study (80 kVp, 250 mA). Images are reconstructed by using AIDR *(A, C, E)* and FBP *(B, D, F).* There is a reduction in image noise and improvement in image quality with AIDR compared with FBP reconstructions.

ation when performing nonenhanced coronary artery calcium scoring examinations, another time-honored quantitative CT imaging application. One study showed decreased noise but also decreased Agatston and volumetric calcium scores due to reduced blooming artifacts when ASIR was used compared with FBP (110,111); the practical implication is that calcium scoring using IR may result in incorrect risk stratification, as the population-based studies that provided calcium score nomograms used FBP reconstructions. In contrast, IR does not appear to significantly alter the analysis of plaque composition and plaque burden quantification (88,112,113).

Abdomen and Pelvis

A number of advantages have been demonstrated with use of IR in abdominal and pelvic imaging. Principle among them is noise reduction, which allows concomitant dose reduction. Routine abdominal and pelvic CT performed with commercially available IR software allows equivalent to improved subjective and objective image quality at dose reductions of 25%–50% compared with full-dose FBP (114–120). Newer IR algorithms have been shown to allow diagnostic quality acquisitions with dose-reduced protocols performed with only 50 mA, providing 75% dose reductions in selected patients compared with standard acquisition parameters (121,122) (Figs 9, 10).

CT angiography.—Like IR in coronary CT angiography, body CT angiographic applications should allow significant dose reductions while maintaining diagnostic image quality (32,123), and model-based IR products may lead to improved accuracy when measuring vascular diameter and evaluating vessel wall attenuation (124).

Liver CT.—IR application in liver CT has been validated in both phantom and in-vivo studies, which have shown that dose reductions between 41% and 50% are possible without sacrificing image quality (125,126). This may be particularly relevant in hepatic perfusion imaging, which has traditionally involved relatively high radiation dose values. A recent study showed that the use of AIDR allowed a 45% dose reduction by applying a tube current of 120 mAs instead of the standard 250 mAs without affecting image quality or quantitative hepatic perfusion values (127).

While IR can increase CNR by reducing noise alone, there has also been interest in improving small lesion conspicuity by further enhancing CNR with combined low-dose acquisition and IR

Figure 9

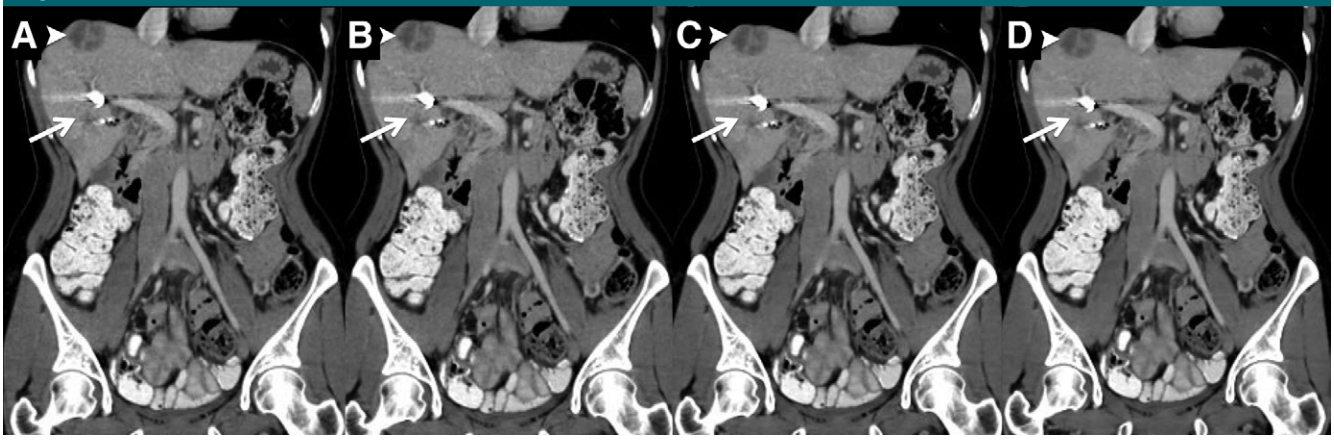

Figure 9: Coronal reformations of contrast-enhanced abdominal CT study in a patient with liver metastasis (arrowhead). Beam-hardening artifacts (arrow) due to metallic clips are seen. Images reconstructed with, *A,* FBP and SAFIRE strengths, *B,* 1, *C,* 3, and, *D,* 5. Increasing the IR strength reduces image noise and beam-hardening artifacts.

Figure 10

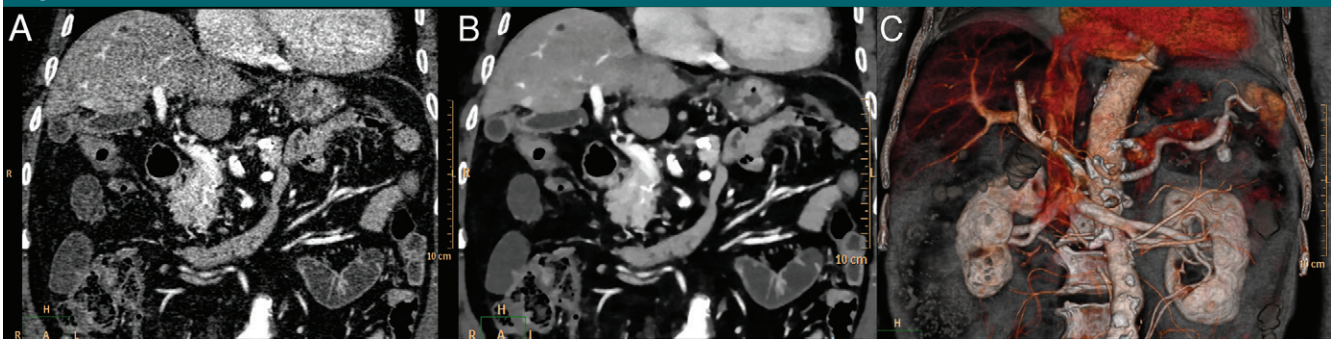

Figure 10: Coronal reformations of CT angiographic study of the abdominal vasculature (effective dose, 2.8 mSv) reconstructed with, *A,* FBP and, *B,* iDose[4]. The IR algorithm reduces image noise *(B)* and improves the image quality of three-dimensional volume-rendered reconstructions *(C).* (Image courtesy of C. Liang, MD, and Z. Liu, MD, Guangdong General Hospital, Guangzhou, China.)

techniques (Fig 11). Lower kilovoltage scans increase attenuation (contrast), while IR mitigates the increased noise associated with these low-dose scans; this approach has been shown to be effective in increasing CNR in low-dose arterial, portal, and late vascular phase image acquisitions (128). While several studies have demonstrated no significant improvement in the detection of small low-contrast liver lesions (129,130), this strategy has been shown to be effective in improving the detection of hypervascular liver lesions such as hepatocellular carcinoma (131). IR-based improvements in subjective image quality and CNR also manifest in CT portovenography, in which significantly improved image quality of volume-rendered images has been demonstrated (132).

CT enterography.—Two studies on patients with Crohn disease have shown that CT enterography with IR can lead to statistically significant dose reductions between 35% and 50% without loss of image quality or observer confidence compared with FBP (133,134).

CT colonography.—CT colonography is becoming a widely recognized screening tool for colorectal cancer. As for all screening application in a priori healthy populations, ionizing radiation exposure should be kept to an absolute minimum. Studies have shown that reduced-dose (25 vs 50 mAs) studies using ASIR have equivalent image quality with decreased noise compared with those using FBP (135), and half-dose reconstructions using SAFIRE produce equivalent image quality as full-dose reconstructions using FBP (136). Furthermore, a porcine colon phantom study comparing FBP, ASIR, and Veo reconstructions at various radiation dose acquisitions showed statistically significant improvement in per-polyp detection sensitivity with use of ASIR and significantly reduced image noise with both IR techniques (137) (Figs 12, 13).

CT urography.—Initial experiences (138,139) have demonstrated that the

Figure 11

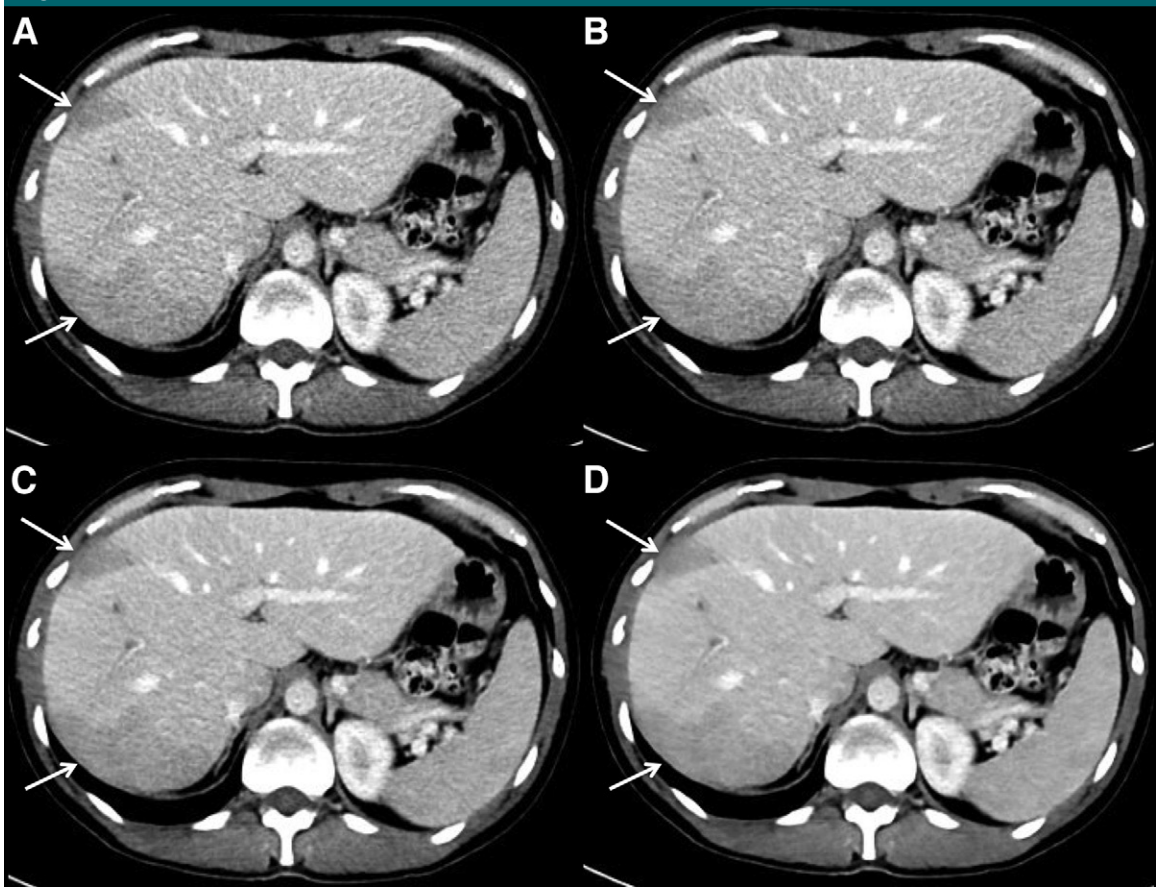

Figure 11: Transverse sections from contrast-enhanced abdominal CT study reconstructed with, *A,* FBP and SAFIRE strengths, *B,* 1, *C,* 3, and, *D,* 5. With increasing IR strength, a reduction in image noise is observed, allowing for better delineation of regional changes in hepatic perfusion (arrows).

in-vivo applications of IR to CT urography allow a significant radiation dose reduction between 45% and 84% without reducing image quality and without affecting diagnostic confidence. Kulkarni et al (139) demonstrated that even when the dose was reduced from 9.9 to 1.8 mGy, images were still deemed diagnostically acceptable for reliable detection of urinary stones. Furthermore, this extreme dose reduction did not impair the evaluation of the rest of the abdomen and pelvis for noncalculus findings.

IR in Pediatric Imaging

The potential stochastic effects of ionizing radiation in pediatric patients have raised considerable concern over the past several years within both the medical and lay press (140,141). Pediatric patients are thought to have increased radiation sensitivity of their immature tissues, generally have a longer life expectancy and therefore more time to develop stochastic effects, and often undergo repeat diagnostic testing. It is no surprise then that there have been strong efforts in limiting ionizing radiation exposure in this population, as, for instance, prominently exemplified by the Image Gently campaign (142). A number of CT techniques have been developed and are emerging, including high-pitch, low-tube-voltage protocols; patient-specific protocol optimization; increased and more effective use of shielding devices; and an overall emphasis on staff training and attention. IR appears to be well suited as an additional tool to provide diagnostic image quality with the lowest doses possible (32,35). An increasing number of studies are reporting that noise, CNR, signal-to-noise ratio, and subjective image quality are significantly improved with the use of IR algorithms in pediatric patients (46,143–146). In pediatric cardiac CT, Han et al (145) reported a significant noise reduction of 34%, and substantial increase of 41% and 56% in CNR and signal-to-noise ratio, respectively, with the use of SAFIRE compared with FBP. Depending on the body region, the potential dose reduction provided by the implementation of IR techniques ranges between 22% and 48% without impairing diagnostic confidence (51,147–149).

Figure 12

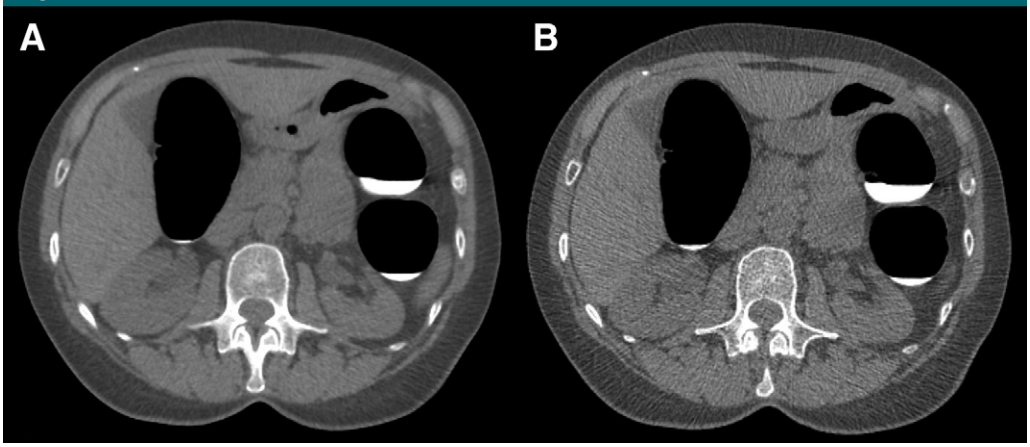

Figure 12: Transverse sections of CT colonography study (80 mAs, 100 kVp) reconstructed with, *A,* 40% ASIR and, *B,* FBP. Application of the ASIR algorithm *(A)* to low-dose CT colonography reduces image noise and improves overall image quality compared with FBP *(B)*.

Figure 13

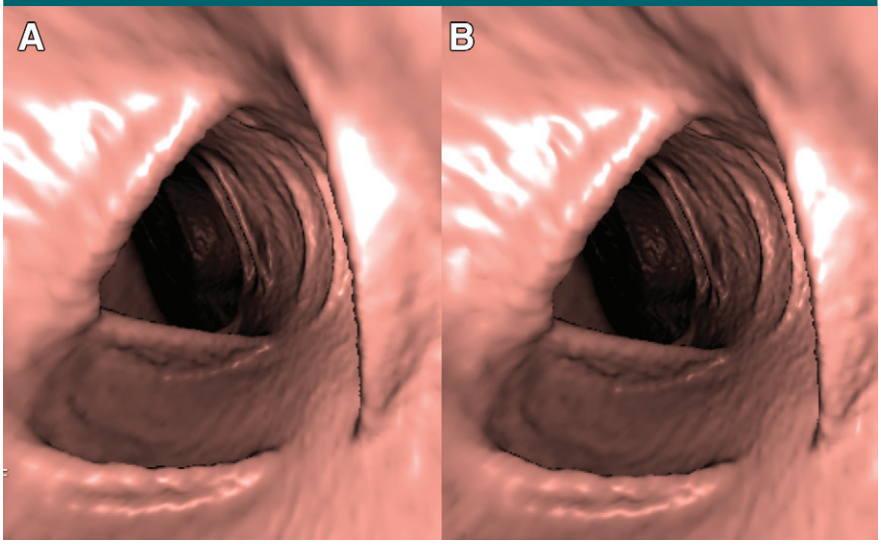

Figure 13: Three-dimensional surface-rendered endoluminal displays of CT colonography study (80 mAs, 100 kVp) reconstructed with, *A,* 40% ASIR and, *B,* FBP. Note that image noise causes a mildly speckled appearance of the colon wall on FBP image *(B)*, which is reduced on ASIR image *(A)*.

IR in Obese Patients

CT examinations in the obese population are challenging. Noise is intrinsically higher secondary to reduced photon transmission and scatter, compromising both image quality and diagnostic accuracy (150,151). Several techniques can improve image quality in obese patients, such as BMI-adaptive scan protocols (generally using higher kilovoltage acquisitions) and half-scan reconstruction techniques using dual-source CT (152,153). Unfortunately, both techniques result in significantly increased radiation dose ($P < .01$). The noise-reduction properties of IR may hold particular appeal in the evaluation of obese individuals, with IR applications showing reductions in both image noise and radiation dose in this population (35,154,155). Kligerman et al (156) demonstrated a significant noise reduction using iDose compared with FBP in obese patients (BMI ≥ 30 kg/m^2) undergoing CT pulmonary angiography. Moreover, the implementation of iDose level 5 provided noise values that were comparable to those in nonobese control subjects (average BMI, 22 kg/m^2). In coronary CT angiography, Wang et al (155) showed a potential dose reduction of 50% facilitated by the use of SAFIRE in obese patients without sacrificing image quality. This is consistent with the results of other studies that have shown radiation dose reductions of 32% and 50% in abdominal-pelvic CT imaging (157) and coronary CT angiography, respectively (158).

IR in Emergency Radiology

IR algorithms have also been deemed effective in emergency conditions. They are able to reduce total radiation dose without any loss in image quality in applications that included acute aortic syndrome (20% decrease in dose length product using ASIR compared with FBP) (123) and trauma surveys of the brain, cervical spine, chest, abdomen, and pelvis (20% dose decrease using ASIR compared with FBP) (49). Importantly, one study also demonstrated that IR implementation (in this study, iDose^4) does not significantly delay reconstruction time or speed (159).

Summary

Increases in available and affordable computer power have fostered the development of a variety of IR algorithms and their application to diagnostic CT imaging. While the specific algorithms differ, the clinical basis for the benefits of IR implementation primarily involves image noise reduction, which leads to improved objective and subjective image quality compared with those using FBP reconstructions. Decreased noise alone results in improved image quality in previously challenging areas, such as ultra-high-resolution imaging and the evaluation of obese individuals. Perhaps more important, the noise-reduction properties of IR techniques hold potential to enable designing CT acquisition protocols at reduced radiation dose levels without sacrificing image quality, which is particularly attractive in screening examinations (eg, lung and colorectal cancer), perfusion studies, pediatric imaging, and for repeat examinations. Besides enhancements in general measures of image quality, an increasing body of evidence describes improvements in the diagnostic accuracy of various CT imaging applications, for example, via artifact reduction, by use of IR techniques. However, while an ever greater number of scientific reports highlight the substantial promise of IR techniques to enhance the diagnostic performance and to incur drastic reductions in radiation requirements at CT, major evidence confirming such initial findings in larger patient populations is still mostly lacking, along with professional society guidelines on the appropriate routine implementation of IR techniques. However, we will likely observe a gradual development of a more meaningful evidence base and of pertinent guidelines with the more widespread availability of IR algorithms and increasing familiarity of the medical imaging community with their use. Refinement of current IR techniques will likely result in more effective and universal clinical adoption, and emerging and future algorithms promise to expand the role of IR to novel diagnostic imaging applications. Overall, it appears safe to predict that in the foreseeable future IR will replace traditional analytical methods as the preferred CT image reconstruction method.

Disclosures of Conflicts of Interest: L.L.G. Activities related to the present article: disclosed no relevant relationships. Activities not related to the present article: received payment for lectures including service on speakers bureaus (year 2012) from GE Healthcare (Germany). Other relationships: disclosed no relevant relationships. **U.J.S.** Activities related to the present article: disclosed no relevant relationships. Activities not related to the present article: reports grants from Bayer, Bracco, GE, Medrad, Siemens, personal fees from Bayer, GE, Siemens, nonfinancial support from Bayer, Medrad, Siemens. Other relationships: disclosed no relevant relationships. **F.G.M.** disclosed no relevant relationships. **J.W.N.** disclosed no relevant relationships. **G.B.** Activities related to the present article: disclosed no relevant relationships. Activities not related to the present article: received speaker honorarium from Bayer and Siemens Healthcare. Other relationships: disclosed no relevant relationships. **J.A.L.** Activities related to the present article: received fees from GE Healthcare. Activities not related to the present article: received payment for service on speakers bureau from GE Healthcare. Other relationships: disclosed no relevant relationships. **N.S.P.** Activities related to the present article: disclosed no relevant relationships. Activities not related to the present article: institution received research grant from Toshiba Medical Systems, author received payment for service on speakers bureau from Toshiba Medical Systems. Other relationships: research collaboration Carestream Healt. **M.R.** disclosed no relevant relationships. **A.L.** disclosed no relevant relationships. **C.N.D.C.** disclosed no relevant relationships.

References

1. Ambrose J. Computerized transverse axial scanning (tomography). II. Clinical application. Br J Radiol 1973;46(552):1023–1047.
2. Hounsfield GN. Computerized transverse axial scanning (tomography). I. Description of system. Br J Radiol 1973;46(552):1016–1022.
3. Boyd DP, Lipton MJ. Cardiac computed tomography. Proc IEEE 1983;71(3):298–307.
4. Kalender WA, Seissler W, Klotz E, Vock P. Spiral volumetric CT with single-breath-hold technique, continuous transport, and continuous scanner rotation. Radiology 1990;176(1):181–183.
5. Klingenbeck-Regn K, Schaller S, Flohr T, Ohnesorge B, Kopp AF, Baum U. Subsecond multi-slice computed tomography: basics and applications. Eur J Radiol 1999;31(2):110–124.
6. McCollough CH, Zink FE. Performance evaluation of a multi-slice CT system. Med Phys 1999;26(11):2223–2230.
7. Hu H. Multi-slice helical CT: scan and reconstruction. Med Phys 1999;26(1):5–18.
8. Zhang D, Li X, Liu B. Objective characterization of GE discovery CT750 HD scanner: gemstone spectral imaging mode. Med Phys 2011;38(3):1178–1188.
9. Hsiao EM, Rybicki FJ, Steigner M. CT coronary angiography: 256-slice and 320-detector row scanners. Curr Cardiol Rep 2010;12(1):68–75.
10. Rybicki FJ, Otero HJ, Steigner ML, et al. Initial evaluation of coronary images from 320-detector row computed tomography. Int J Cardiovasc Imaging 2008;24(5):535–546.
11. Flohr TG, McCollough CH, Bruder H, et al. First performance evaluation of a dual-source CT (DSCT) system. Eur Radiol 2006;16(2):256–268.
12. Brooks RA, Di Chiro G. Principles of computer assisted tomography (CAT) in radiographic and radioisotopic imaging. Phys Med Biol 1976;21(5):689–732.
13. Andersen AH, Kak AC. Simultaneous algebraic reconstruction technique (SART): a superior implementation of the art algorithm. Ultrason Imaging 1984;6(1):81–94.
14. Gordon R, Bender R, Herman GT. Algebraic reconstruction techniques (ART) for three-dimensional electron microscopy and x-ray photography. J Theor Biol 1970;29(3):471–481.
15. Gilbert P. Iterative methods for the three-dimensional reconstruction of an object from projections. J Theor Biol 1972;36(1):105–117.
16. Hsieh J. Adaptive statistical iterative reconstruction: GE white paper. Waukesha, Wis: GE Healthcare, 2008.
17. Cheng L, Chen Y, Fang T, Tyan J. Fast iterative adaptive reconstruction in low-dose CT imaging. In: 2006 IEEE International Conference on Image Processing, 2006; 889–892.
18. Hara AK, Paden RG, Silva AC, Kujak JL, Lawder HJ, Pavlicek W. Iterative reconstruction technique for reducing body radiation dose at CT: feasibility study. AJR Am J Roentgenol 2009;193(3):764–771.
19. Liu YJ, Zhu PP, Chen B, et al. A new iterative algorithm to reconstruct the refractive index. Phys Med Biol 2007;52(12):L5–L13.
20. Nuyts J, De Man B, Dupont P, Defrise M, Suetens P, Mortelmans L. Iterative reconstruction for helical CT: a simulation study. Phys Med Biol 1998;43(4):729–737.
21. Paden RG, Pavlicek W, Peter MB, Boltz TF II, Park K, Langan DA. Adaptive statistical iterative reconstruction (ASIR) for CT dose reduction of head and body examinations: a phantom study [abstr]. In: Radiological Society of North America Scientific Assembly and Annual Meeting Program. Oak Brook, Ill: Radiological Society of North America, 2008, 455.
22. Leipsic J, Labounty TM, Heilbron B, et al. Adaptive statistical iterative reconstruction: assessment of image noise and image qual-

ity in coronary CT angiography. AJR Am J Roentgenol 2010;195(3):649–654.

23. Mueck FG, Körner M, Scherr MK, et al. Upgrade to iterative image reconstruction (IR) in abdominal MDCT imaging: a clinical study for detailed parameter optimization beyond vendor recommendations using the adaptive statistical iterative reconstruction environment (ASIR). Rofo 2012;184(3):229–238.

24. Thibault J-B. Veo: CT model-based iterative reconstruction. *http://www.gehealthcare.com*. Published 2010. Accessed September 2013.

25. Yu Z, Thibault JB, Bouman CA, Sauer KD, Hsieh J. Fast model-based X-ray CT reconstruction using spatially nonhomogeneous ICD optimization. IEEE Trans Image Process 2011;20(1): 161–175.

26. Thibault JB, Sauer KD, Bouman CA, Hsieh J. A three-dimensional statistical approach to improved image quality for multislice helical CT. Med Phys 2007;34(11):4526–4544.

27. Nelson RC, Feuerlein S, Boll DT. New iterative reconstruction techniques for cardiovascular computed tomography: how do they work, and what are the advantages and disadvantages? J Cardiovasc Comput Tomogr 2011;5(5): 286–292.

28. Laqmani A, Buhk JH, Henes FO, et al. Impact of a 4th generation iterative reconstruction technique on image quality in low-dose computed tomography of the chest in immunocompromised patients. Rofo 2013;185(8): 749–757.

29. Willemink MJ, Borstlap J, Takx RA, et al. The effects of computed tomography with iterative reconstruction on solid pulmonary nodule volume quantification. PLoS ONE 2013;8(2): e58053.

30. Mehta D, Thompson R, Morton T, Dhanantwari A, Shefer E. Iterative model reconstruction: simultaneously lowered computed tomography radiation dose and improved image quality. Med Phys Int 2013;1(2):147–155.

31. Grant K, Flohr T. Iterative reconstruction in image space (IRIS). *http://www.usa.siemens.com/healthcare*. Published 2010. Accessed September 2013.

32. Winklehner A, Karlo C, Puippe G, et al. Raw data-based iterative reconstruction in body CTA: evaluation of radiation dose saving potential. Eur Radiol 2011;21(12):2521–2526.

33. Baumueller S, Winklehner A, Karlo C, et al. Low-dose CT of the lung: potential value of iterative reconstructions. Eur Radiol 2012;22(12): 2597–2606.

34. Grant K, Raupach R. SAFIRE: Sinogram affirmed iterative reconstruction. *http://www.usa.siemens.com/healthcare*. Published 2012. Accessed September 2013.

35. Moscariello A, Takx RA, Schoepf UJ, et al. Coronary CT angiography: image quality, diagnostic accuracy, and potential for radiation dose reduction using a novel iterative image reconstruction technique-comparison with traditional filtered back projection. Eur Radiol 2011;21(10):2130–2138.

36. Gordic S, Morsbach F, Schmidt B, et al. Ultralow-dose chest computed tomography for pulmonary nodule detection: first performance evaluation of single energy scanning with spectral shaping. Invest Radiol 2014;49(7): 465–473.

37. Gervaise A, Osemont B, Lecocq S, et al. CT image quality improvement using adaptive iterative dose reduction with wide-volume acquisition on 320-detector CT. Eur Radiol 2012; 22(2):295–301.

38. Tatsugami F, Matsuki M, Nakai G, et al. The effect of adaptive iterative dose reduction on image quality in 320-detector row CT coronary angiography. Br J Radiol 2012;85(1016): e378–e382.

39. Irwan R, Nakanishi S, Blum A. AIDR 3D: reduces dose and simultaneously improves image quality. *https://www.toshiba-medical.eu/eu/wp-content/uploads/sites/2/2014/10/AIDR-3D-white-paper1.pdf*. Published 2011. Accessed September 2013.

40. Yang Z, Zamyatin AA, Akino N. Effective data-domain noise and streak reduction for x-ray CT. In: Kachelriess M, Rafecas M, eds. The 11th International Meeting on Fully 3D Image Reconstruction in Radiology and Nuclear Medicine. Potsdam, Germany, 2011; 290–293. *http://www.fully3d.org/2011/Fully-3D2011Proceedings.pdf*.

41. Yang Z, Silver MD, Yasuhiro N. Adpative weight anisotropic diffusion for computed tomography denoising. In: Kachelriess M, Rafecas M, eds. The 11th International Meeting on Fully 3D Image Reconstruction in Radiology and Nuclear Medicine. Potsdam, Germany, 2011; 210–213. *http://www.fully3d.org/2011/Fully3D2011Proceedings.pdf*.

42. Tack D, Jahnen A, Kohler S, et al. Multidetector CT radiation dose optimisation in adults: short- and long-term effects of a clinical audit. Eur Radiol 2014;24(1):169–175.

43. Bankier AA, Kressel HY. Through the Looking Glass revisited: the need for more meaning and less drama in the reporting of dose and dose reduction in CT. Radiology 2012;265(1):4–8.

44. Ghetti C, Ortenzia O, Serreli G. CT iterative reconstruction in image space: a phantom study. Phys Med 2012;28(2):161–165.

45. Ghetti C, Palleri F, Serreli G, Ortenzia O, Ruffini L. Physical characterization of a new CT iterative reconstruction method operating in sinogram space. J Appl Clin Med Phys 2013;14(4):4347.

46. Noël PB, Fingerle AA, Renger B, Münzel D, Rummeny EJ, Dobritz M. Initial performance characterization of a clinical noise-suppressing reconstruction algorithm for MDCT. AJR Am J Roentgenol 2011;197(6):1404–1409.

47. Miéville FA, Gudinchet F, Brunelle F, Bochud FO, Verdun FR. Iterative reconstruction methods in two different MDCT scanners: physical metrics and 4-alternative forced-choice detectability experiments—a phantom approach. Phys Med 2013;29(1):99–110.

48. Geyer LL, Körner M, Hempel R, et al. Evaluation of a dedicated MDCT protocol using iterative image reconstruction after cervical spine trauma. Clin Radiol 2013;68(7):e391–e396.

49. Maxfield MW, Schuster KM, McGillicuddy EA, et al. Impact of adaptive statistical iterative reconstruction on radiation dose in evaluation of trauma patients. J Trauma Acute Care Surg 2012;73(6):1406–1411.

50. Kilic K, Erbas G, Guryildirim M, Arac M, Ilgit E, Coskun B. Lowering the dose in head CT using adaptive statistical iterative reconstruction. AJNR Am J Neuroradiol 2011;32(9): 1578–1582.

51. Kilic K, Erbas G, Guryildirim M, et al. Quantitative and qualitative comparison of standard-dose and low-dose pediatric head computed tomography: a retrospective study assessing the effect of adaptive statistical iterative reconstruction. J Comput Assist Tomogr 2013;37(3):377–381.

52. Korn A, Bender B, Fenchel M, et al. Sinogram affirmed iterative reconstruction in head CT: improvement of objective and subjective image quality with concomitant radiation dose reduction. Eur J Radiol 2013;82(9):1431–1435.

53. Korn A, Fenchel M, Bender B, et al. Iterative reconstruction in head CT: image quality of routine and low-dose protocols in comparison with standard filtered back-projection. AJNR Am J Neuroradiol 2012;33(2):218–224.

54. Wu TH, Hung SC, Sun JY, et al. How far can the radiation dose be lowered in head CT with iterative reconstruction? analysis of imaging quality and diagnostic accuracy. Eur Radiol 2013;23(9):2612–2621.

55. Lin CJ, Wu TH, Lin CH, et al. Can iterative reconstruction improve imaging quality for lower radiation CT perfusion? initial experience. AJNR Am J Neuroradiol 2013;34(8): 1516–1521.

56. Machida H, Takeuchi H, Tanaka I, et al. Improved delineation of arteries in the posterior fossa of the brain by model-based iterative reconstruction in volume-rendered 3D CT angiography. AJNR Am J Neuroradiol 2013;34(5): 971–975.

57. Machida H, Tanaka I, Fukui R, et al. Improved delineation of the anterior spinal artery with model-based iterative reconstruction in CT angiography: a clinical pilot study. AJR Am J Roentgenol 2013;200(2):442–446.

58. Nishida J, Kitagawa K, Nagata M, Yamazaki A, Nagasawa N, Sakuma H. Model-based iterative reconstruction for multi-detector row CT assessment of the Adamkiewicz artery. Radiology 2014;270(1):282–291.

59. Becce F, Ben Salah Y, Verdun FR, et al. Computed tomography of the cervical spine: comparison of image quality between a standard-dose and a low-dose protocol using filtered

back-projection and iterative reconstruction. Skeletal Radiol 2013;42(7):937–945.

60. Omoumi P, Verdun FR, Ben Salah Y, et al. Low-dose multidetector computed tomography of the cervical spine: optimization of iterative reconstruction strength levels. Acta Radiol 2014;55(3):335–344.

61. Schulz B, Beeres M, Bodelle B, et al. Performance of iterative image reconstruction in CT of the paranasal sinuses: a phantom study. AJNR Am J Neuroradiol 2013;34(5):1072–1076.

62. Niu YT, Mehta D, Zhang ZR, et al. Radiation dose reduction in temporal bone CT with iterative reconstruction technique. AJNR Am J Neuroradiol 2012;33(6):1020–1026.

63. Rapalino O, Kamalian S, Kamalian S, et al. Cranial CT with adaptive statistical iterative reconstruction: improved image quality with concomitant radiation dose reduction. AJNR Am J Neuroradiol 2012;33(4):609–615.

64. Katsura M, Sato J, Akahane M, et al. Comparison of pure and hybrid iterative reconstruction techniques with conventional filtered back projection: image quality assessment in the cervicothoracic region. Eur J Radiol 2013;82(2):356–360.

65. Morsbach F, Wurnig M, Kunz DM, et al. Metal artefact reduction from dental hardware in carotid CT angiography using iterative reconstructions. Eur Radiol 2013;23(10):2687–2694.

66. Pontana F, Pagniez J, Flohr T, et al. Chest computed tomography using iterative reconstruction vs filtered back projection. I. Evaluation of image noise reduction in 32 patients. Eur Radiol 2011;21(3):627–635.

67. Singh S, Kalra MK, Gilman MD, et al. Adaptive statistical iterative reconstruction technique for radiation dose reduction in chest CT: a pilot study. Radiology 2011;259(2):565–573.

68. Hwang HJ, Seo JB, Lee HJ, et al. Low-dose chest computed tomography with sinogram-affirmed iterative reconstruction, iterative reconstruction in image space, and filtered back projection: studies on image quality. J Comput Assist Tomogr 2013;37(4):610–617.

69. Kalra MK, Woisetschläger M, Dahlström N, et al. Sinogram-affirmed iterative reconstruction of low-dose chest CT: effect on image quality and radiation dose. AJR Am J Roentgenol 2013;201(2):W235–W244.

70. Leipsic J, Nguyen G, Brown J, Sin D, Mayo JR. A prospective evaluation of dose reduction and image quality in chest CT using adaptive statistical iterative reconstruction. AJR Am J Roentgenol 2010;195(5):1095–1099.

71. Vardhanabhuti V, Loader RJ, Mitchell GR, Riordan RD, Roobottom CA. Image quality assessment of standard- and low-dose chest CT using filtered back projection, adaptive statistical iterative reconstruction, and novel model-based iterative reconstruction algorithms. AJR Am J Roentgenol 2013;200(3):545–552.

72. Yamada Y, Jinzaki M, Hosokawa T, et al. Dose reduction in chest CT: comparison of the adaptive iterative dose reduction 3D, adaptive iterative dose reduction, and filtered back projection reconstruction techniques. Eur J Radiol 2012;81(12):4185–4195.

73. Ichikawa Y, Kitagawa K, Nagasawa N, Murashima S, Sakuma H. CT of the chest with model-based, fully iterative reconstruction: comparison with adaptive statistical iterative reconstruction. BMC Med Imaging 2013;13(1):27.

74. Neroladaki A, Botsikas D, Boudabbous S, Becker CD, Montet X. Computed tomography of the chest with model-based iterative reconstruction using a radiation exposure similar to chest x-ray examination: preliminary observations. Eur Radiol 2013;23(2):360–366.

75. Wang H, Tan B, Zhao B, Liang C, Xu Z. Raw-data-based iterative reconstruction versus filtered back projection: image quality of low-dose chest computed tomography examinations in 87 patients. Clin Imaging 2013;37(6):1024–1032.

76. Botelho MP, Agrawal R, Gonzalez-Guindalini FD, et al. Effect of radiation dose and iterative reconstruction on lung lesion conspicuity at MDCT: does one size fit all? Eur J Radiol 2013;82(11):e726–e733.

77. Prakash P, Kalra MK, Ackman JB, et al. Diffuse lung disease: CT of the chest with adaptive statistical iterative reconstruction technique. Radiology 2010;256(1):261–269.

78. Miéville FA, Berteloot L, Grandjean A, et al. Model-based iterative reconstruction in pediatric chest CT: assessment of image quality in a prospective study of children with cystic fibrosis. Pediatr Radiol 2013;43(5):558–567.

79. Nishio M, Matsumoto S, Ohno Y, et al. Emphysema quantification by low-dose CT: potential impact of adaptive iterative dose reduction using 3D processing. AJR Am J Roentgenol 2012;199(3):595–601.

80. Mets OM, de Jong PA, van Ginneken B, Gietema HA, Lammers JW. Quantitative computed tomography in COPD: possibilities and limitations. Lung 2012;190(2):133–145.

81. Willemink MJ, Leiner T, Budde RP, et al. Systematic error in lung nodule volumetry: effect of iterative reconstruction versus filtered back projection at different CT parameters. AJR Am J Roentgenol 2012;199(6):1241–1246.

82. Wielpütz MO, Lederlin M, Wroblewski J, et al. CT volumetry of artificial pulmonary nodules using an ex vivo lung phantom: influence of exposure parameters and iterative reconstruction on reproducibility. Eur J Radiol 2013;82(9):1577–1583.

83. Yanagawa M, Honda O, Kikuyama A, et al. Pulmonary nodules: effect of adaptive statistical iterative reconstruction (ASIR) technique on performance of a computer-aided detection (CAD) system-comparison of performance between different-dose CT scans. Eur J Radiol 2012;81(10):2877–2886.

84. Higuchi K, Nagao M, Matsuo Y, et al. Detection of ground-glass opacities by use of hybrid iterative reconstruction (iDose) and low-dose 256-section computed tomography: a phantom study. Radiol Phys Technol 2013;6(2):299–304.

85. Katsura M, Matsuda I, Akahane M, et al. Model-based iterative reconstruction technique for ultralow-dose chest CT: comparison of pulmonary nodule detectability with the adaptive statistical iterative reconstruction technique. Invest Radiol 2013;48(4):206–212.

86. Yuan R, Shuman WP, Earls JP, et al. Reduced iodine load at CT pulmonary angiography with dual-energy monochromatic imaging: comparison with standard CT pulmonary angiography—a prospective randomized trial. Radiology 2012;262(1):290–297.

87. Leipsic J, Labounty TM, Heilbron B, et al. Estimated radiation dose reduction using adaptive statistical iterative reconstruction in coronary CT angiography: the ERASIR study. AJR Am J Roentgenol 2010;195(3):655–660.

88. Fuchs TA, Fiechter M, Gebhard C, et al. CT coronary angiography: impact of adapted statistical iterative reconstruction (ASIR) on coronary stenosis and plaque composition analysis. Int J Cardiovasc Imaging 2013;29(3):719–724.

89. Gosling O, Loader R, Venables P, et al. A comparison of radiation doses between state-of-the-art multislice CT coronary angiography with iterative reconstruction, multislice CT coronary angiography with standard filtered back-projection and invasive diagnostic coronary angiography. Heart 2010;96(12):922–926.

90. Hou Y, Liu X, Xv S, Guo W, Guo Q. Comparisons of image quality and radiation dose between iterative reconstruction and filtered back projection reconstruction algorithms in 256-MDCT coronary angiography. AJR Am J Roentgenol 2012;199(3):588–594.

91. Hou Y, Xu S, Guo W, Vembar M, Guo Q. The optimal dose reduction level using iterative reconstruction with prospective ECG-triggered coronary CTA using 256-slice MDCT. Eur J Radiol 2012;81(12):3905–3911.

92. Park EA, Lee W, Kim KW, et al. Iterative reconstruction of dual-source coronary CT angiography: assessment of image quality and radiation dose. Int J Cardiovasc Imaging 2012;28(7):1775–1786.

93. Renker M, Ramachandra A, Schoepf UJ, et al. Iterative image reconstruction techniques: applications for cardiac CT. J Cardiovasc Comput Tomogr 2011;5(4):225–230.

94. Schuhbaeck A, Achenbach S, Layritz C, et al. Image quality of ultra-low radiation exposure coronary CT angiography with an effective dose <0.1 mSv using high-pitch spiral acquisition and raw data-based iterative reconstruction. Eur Radiol 2013;23(3):597–606.

95. Yoo RE, Park EA, Lee W, et al. Image quality of adaptive iterative dose reduction 3D of coronary CT angiography of 640-slice CT:

comparison with filtered back-projection. Int J Cardiovasc Imaging 2013;29(3):669–676.

96. Yin WH, Lu B, Hou ZH, et al. Detection of coronary artery stenosis with sub-milliSievert radiation dose by prospectively ECG-triggered high-pitch spiral CT angiography and iterative reconstruction. Eur Radiol 2013;23(11):2927–2933.

97. Chen MY, Steigner ML, Leung SW, et al. Simulated 50 % radiation dose reduction in coronary CT angiography using adaptive iterative dose reduction in three-dimensions (AIDR3D). Int J Cardiovasc Imaging 2013;29(5):1167–1175.

98. Pontone G, Andreini D, Bartorelli AL, et al. Feasibility and diagnostic accuracy of a low radiation exposure protocol for prospective ECG-triggering coronary MDCT angiography. Clin Radiol 2012;67(3):207–215.

99. Takx RA, Schoepf UJ, Moscariello A, et al. Coronary CT angiography: comparison of a novel iterative reconstruction with filtered back projection for reconstruction of low-dose CT-Initial experience. Eur J Radiol 2013;82(2):275–280.

100. Hosch W, Stiller W, Mueller D, et al. Reduction of radiation exposure and improvement of image quality with BMI-adapted prospective cardiac computed tomography and iterative reconstruction. Eur J Radiol 2012;81(11):3568–3576.

101. Shen J, Du X, Guo D, et al. Noise-based tube current reduction method with iterative reconstruction for reduction of radiation exposure in coronary CT angiography. Eur J Radiol 2013;82(2):349–355.

102. Yin WH, Lu B, Li N, et al. Iterative reconstruction to preserve image quality and diagnostic accuracy at reduced radiation dose in coronary CT angiography: an intraindividual comparison. JACC Cardiovasc Imaging 2013;6(12):1239–1249.

103. Ebersberger U, Tricarico F, Schoepf UJ, et al. CT evaluation of coronary artery stents with iterative image reconstruction: improvements in image quality and potential for radiation dose reduction. Eur Radiol 2013;23(1):125–132.

104. Eisentopf J, Achenbach S, Ulzheimer S, et al. Low-dose dual-source CT angiography with iterative reconstruction for coronary artery stent evaluation. JACC Cardiovasc Imaging 2013;6(4):458–465.

105. Gebhard C, Fiechter M, Fuchs TA, et al. Coronary artery stents: influence of adaptive statistical iterative reconstruction on image quality using 64-HDCT. Eur Heart J Cardiovasc Imaging 2013;14(10):969–977.

106. Funama Y, Oda S, Utsunomiya D, et al. Coronary artery stent evaluation by combining iterative reconstruction and high-resolution kernel at coronary CT angiography. Acad Radiol 2012;19(11):1324–1331.

107. Min JK, Swaminathan RV, Vass M, Gallagher S, Weinsaft JW. High-definition multidetector computed tomography for evaluation of coronary artery stents: comparison to standard-definition 64-detector row computed tomography. J Cardiovasc Comput Tomogr 2009;3(4):246–251.

108. Oda S, Utsunomiya D, Funama Y, et al. Improved coronary in-stent visualization using a combined high-resolution kernel and a hybrid iterative reconstruction technique at 256-slice cardiac CT-Pilot study. Eur J Radiol 2013;82(2):288–295.

109. Renker M, Nance JW Jr, Schoepf UJ, et al. Evaluation of heavily calcified vessels with coronary CT angiography: comparison of iterative and filtered back projection image reconstruction. Radiology 2011;260(2):390–399.

110. Gebhard C, Fiechter M, Fuchs TA, et al. Coronary artery calcium scoring: influence of adaptive statistical iterative reconstruction using 64-MDCT. Int J Cardiol 2013;167(6):2932–2937.

111. Kurata A, Dharampal A, Dedic A, et al. Impact of iterative reconstruction on CT coronary calcium quantification. Eur Radiol 2013;23(12):3246–3252.

112. Stolzmann P, Schlett CL, Maurovich-Horvat P, et al. Variability and accuracy of coronary CT angiography including use of iterative reconstruction algorithms for plaque burden assessment as compared with intravascular ultrasound-an ex vivo study. Eur Radiol 2012;22(10):2067–2075.

113. Takx RA, Willemink MJ, Nathoe HM, et al. The effect of iterative reconstruction on quantitative computed tomography assessment of coronary plaque composition. Int J Cardiovasc Imaging 2014;30(1):155–163.

114. Deák Z, Grimm JM, Treitl M, et al. Filtered back projection, adaptive statistical iterative reconstruction, and a model-based iterative reconstruction in abdominal CT: an experimental clinical study. Radiology 2013;266(1):197–206.

115. Desai GS, Thabet A, Elias AY, Sahani DV. Comparative assessment of three image reconstruction techniques for image quality and radiation dose in patients undergoing abdominopelvic multidetector CT examinations. Br J Radiol 2013;86(1021):20120161.

116. Karpitschka M, Augart D, Becker HC, Reiser M, Graser A. Dose reduction in oncological staging multidetector CT: effect of iterative reconstruction. Br J Radiol 2013;86(1021):20120224.

117. May MS, Wüst W, Brand M, et al. Dose reduction in abdominal computed tomography: intraindividual comparison of image quality of full-dose standard and half-dose iterative reconstructions with dual-source computed tomography. Invest Radiol 2011;46(7):465–470.

118. Prakash P, Kalra MK, Kambadakone AK, et al. Reducing abdominal CT radiation dose with adaptive statistical iterative reconstruction technique. Invest Radiol 2010;45(4):202–210.

119. Singh S, Kalra MK, Hsieh J, et al. Abdominal CT: comparison of adaptive statistical iterative and filtered back projection reconstruction techniques. Radiology 2010;257(2):373–383.

120. Fletcher JG, Krueger WR, Hough DM, et al. Pilot study of detection, radiologist confidence and image quality with sinogram-affirmed iterative reconstruction at half-routine dose level. J Comput Assist Tomogr 2013;37(2):203–211.

121. Kalra MK, Woisetschläger M, Dahlström N, et al. Radiation dose reduction with sinogram affirmed iterative reconstruction technique for abdominal computed tomography. J Comput Assist Tomogr 2012;36(3):339–346.

122. Singh S, Kalra MK, Do S, et al. Comparison of hybrid and pure iterative reconstruction techniques with conventional filtered back projection: dose reduction potential in the abdomen. J Comput Assist Tomogr 2012;36(3):347–353.

123. Cornfeld D, Israel G, Detroy E, Bokhari J, Mojibian H. Impact of adaptive statistical iterative reconstruction (ASIR) on radiation dose and image quality in aortic dissection studies: a qualitative and quantitative analysis. AJR Am J Roentgenol 2011;196(3):W336–W340.

124. Suzuki S, Machida H, Tanaka I, Ueno E. Measurement of vascular wall attenuation: comparison of CT angiography using model-based iterative reconstruction with standard filtered back-projection algorithm CT in vitro. Eur J Radiol 2012;81(11):3348–3353.

125. Husarik DB, Marin D, Samei E, et al. Radiation dose reduction in abdominal computed tomography during the late hepatic arterial phase using a model-based iterative reconstruction algorithm: how low can we go? Invest Radiol 2012;47(8):468–474.

126. Mitsumori LM, Shuman WP, Busey JM, Kolokythas O, Koprowicz KM. Adaptive statistical iterative reconstruction versus filtered back projection in the same patient: 64 channel liver CT image quality and patient radiation dose. Eur Radiol 2012;22(1):138–143.

127. Negi N, Yoshikawa T, Ohno Y, et al. Hepatic CT perfusion measurements: a feasibility study for radiation dose reduction using new image reconstruction method. Eur J Radiol 2012;81(11):3048–3054.

128. Marin D, Nelson RC, Schindera ST, et al. Low-tube-voltage, high-tube-current multidetector abdominal CT: improved image quality and decreased radiation dose with adaptive statistical iterative reconstruction algorithm—initial clinical experience. Radiology 2010;254(1):145–153.

129. Dobeli KL, Lewis SJ, Meikle SR, Thiele DL, Brennan PC. Noise-reducing algorithms do not necessarily provide superior dose optimisation for hepatic lesion detection with multidetector CT. Br J Radiol 2013;86(1023):20120500.

130. Baker ME, Dong F, Primak A, et al. Contrast-to-noise ratio and low-contrast object resolution on full- and low-dose MDCT: SAFIRE versus fil-

tered back projection in a low-contrast object phantom and in the liver. AJR Am J Roentgenol 2012;199(1):8–18.

131. Hur S, Lee JM, Kim SJ, Park JH, Han JK, Choi BI. 80-kVp CT using iterative reconstruction in image space algorithm for the detection of hypervascular hepatocellular carcinoma: phantom and initial clinical experience. Korean J Radiol 2012;13(2):152–164.

132. Matsuda I, Hanaoka S, Akahane M, et al. Adaptive statistical iterative reconstruction for volume-rendered computed tomography portovenography: improvement of image quality. Jpn J Radiol 2010;28(9):700–706.

133. Kambadakone AR, Chaudhary NA, Desai GS, Nguyen DD, Kulkarni NM, Sahani DV. Low-dose MDCT and CT enterography of patients with Crohn disease: feasibility of adaptive statistical iterative reconstruction. AJR Am J Roentgenol 2011;196(6):W743–W752.

134. Lee SJ, Park SH, Kim AY, et al. A prospective comparison of standard-dose CT enterography and 50% reduced-dose CT enterography with and without noise reduction for evaluating Crohn disease. AJR Am J Roentgenol 2011;197(1):50–57.

135. Flicek KT, Hara AK, Silva AC, Wu Q, Peter MB, Johnson CD. Reducing the radiation dose for CT colonography using adaptive statistical iterative reconstruction: a pilot study. AJR Am J Roentgenol 2010;195(1):126–131.

136. Fletcher JG, Grant KL, Fidler JL, et al. Validation of dual-source single-tube reconstruction as a method to obtain half-dose images to evaluate radiation dose and noise reduction: phantom and human assessment using CT colonography and sinogram-affirmed iterative reconstruction (SAFIRE). J Comput Assist Tomogr 2012;36(5):560–569.

137. Yoon MA, Kim SH, Lee JM, et al. Adaptive statistical iterative reconstruction and Veo: assessment of image quality and diagnostic performance in CT colonography at various radiation doses. J Comput Assist Tomogr 2012;36(5):596–601.

138. Juri H, Matsuki M, Itou Y, et al. Initial experience with adaptive iterative dose reduction 3D to reduce radiation dose in computed tomographic urography. J Comput Assist Tomogr 2013;37(1):52–57.

139. Kulkarni NM, Uppot RN, Eisner BH, Sahani DV. Radiation dose reduction at multidetector CT with adaptive statistical iterative reconstruction for evaluation of urolithiasis: how low can we go? Radiology 2012;265(1):158–166.

140. Pearce MS, Salotti JA, Little MP, et al. Radiation exposure from CT scans in childhood and subsequent risk of leukaemia and brain tumours: a retrospective cohort study. Lancet 2012;380(9840):499–505.

141. Mathews JD, Forsythe AV, Brady Z, et al. Cancer risk in 680,000 people exposed to computed tomography scans in childhood or adolescence: data linkage study of 11 million Australians. BMJ 2013;346:f2360.

142. Goske MJ, Applegate KE, Boylan J, et al. The Image Gently campaign: working together to change practice. AJR Am J Roentgenol 2008;190(2):273–274.

143. Scheffel H, Stolzmann P, Schlett CL, et al. Coronary artery plaques: cardiac CT with model-based and adaptive-statistical iterative reconstruction technique. Eur J Radiol 2012;81(3):e363–e369.

144. Utsunomiya D, Weigold WG, Weissman G, Taylor AJ. Effect of hybrid iterative reconstruction technique on quantitative and qualitative image analysis at 256-slice prospective gating cardiac CT. Eur Radiol 2012;22(6):1287–1294.

145. Han BK, Grant KL, Garberich R, Sedlmair M, Lindberg J, Lesser JR. Assessment of an iterative reconstruction algorithm (SAFIRE) on image quality in pediatric cardiac CT datasets. J Cardiovasc Comput Tomogr 2012;6(3):200–204.

146. Tricarico F, Hlavacek AM, Schoepf UJ, et al. Cardiovascular CT angiography in neonates and children: image quality and potential for radiation dose reduction with iterative image reconstruction techniques. Eur Radiol 2013;23(5):1306–1315.

147. Brady SL, Yee BS, Kaufman RA. Characterization of adaptive statistical iterative reconstruction algorithm for dose reduction in CT: a pediatric oncology perspective. Med Phys 2012;39(9):5520–5531.

148. Singh S, Kalra MK, Shenoy-Bhangle AS, et al. Radiation dose reduction with hybrid iterative reconstruction for pediatric CT. Radiology 2012;263(2):537–546.

149. Vorona GA, Zuccoli G, Sutcavage T, Clayton BL, Ceschin RC, Panigrahy A. The use of adaptive statistical iterative reconstruction in pediatric head CT: a feasibility study. AJNR Am J Neuroradiol 2013;34(1):205–211.

150. Raff GL, Gallagher MJ, O'Neill WW, Goldstein JA. Diagnostic accuracy of noninvasive coronary angiography using 64-slice spiral computed tomography. J Am Coll Cardiol 2005;46(3):552–557.

151. Alkadhi H, Scheffel H, Desbiolles L, et al. Dual-source computed tomography coronary angiography: influence of obesity, calcium load, and heart rate on diagnostic accuracy. Eur Heart J 2008;29(6):766–776.

152. Leschka S, Stinn B, Schmid F, et al. Dual source CT coronary angiography in severely obese patients: trading off temporal resolution and image noise. Invest Radiol 2009;44(11):720–727.

153. Chinnaiyan KM, McCullough PA, Flohr TG, Wegner JH, Raff GL. Improved noninvasive coronary angiography in morbidly obese patients with dual-source computed tomography. J Cardiovasc Comput Tomogr 2009;3(1):35–42.

154. Renker M, Geyer LL, Krazinski AW, Silverman JR, Ebersberger U, Schoepf UJ. Iterative image reconstruction: a realistic dose-saving method in cardiac CT imaging? Expert Rev Cardiovasc Ther 2013;11(4):403–409.

155. Wang R, Schoepf UJ, Wu R, et al. Image quality and radiation dose of low dose coronary CT angiography in obese patients: sinogram affirmed iterative reconstruction versus filtered back projection. Eur J Radiol 2012;81(11):3141–3145.

156. Kligerman S, Mehta D, Farnadesh M, Jeudy J, Olsen K, White C. Use of a hybrid iterative reconstruction technique to reduce image noise and improve image quality in obese patients undergoing computed tomographic pulmonary angiography. J Thorac Imaging 2013;28(1):49–59.

157. Desai GS, Uppot RN, Yu EW, Kambadakone AR, Sahani DV. Impact of iterative reconstruction on image quality and radiation dose in multidetector CT of large body size adults. Eur Radiol 2012;22(8):1631–1640.

158. Gebhard C, Fuchs TA, Fiechter M, et al. Image quality of low-dose CCTA in obese patients: impact of high-definition computed tomography and adaptive statistical iterative reconstruction. Int J Cardiovasc Imaging 2013;29(7):1565–1574.

159. Willemink MJ, Schilham AM, Leiner T, Mali WP, de Jong PA, Budde RP. Iterative reconstruction does not substantially delay CT imaging in an emergency setting. Insights Imaging 2013;4(3):391–397.